Received: 22 December 2021 | Revised: 9 November 2022 | Accepted: 14 December 2022

DOI: 10.1111/gcbb.13024

GCB-BIOENERGY BIOPRODUCTS FOR A SUSTAINABLE BIOECONOMY Open Access

WILEY

RESEARCH ARTICLE

Global warming intensity of biofuel derived from switchgrass grown on marginal land in Michigan

Seungdo Kim[1,2] | **Bruce E. Dale**[1,2] | **Rafael Martinez-Feria**[1,3] | **Bruno Basso**[1,3,4] | **Kurt Thelen**[1,5] | **Christos T. Maravelias**[6,7,8] | **Douglas Landis**[1,9] | **Tyler J. Lark**[8,10] | **G. Philip Robertson**[1,4,11]

[1]DOE Great Lakes Bioenergy Research Center, Michigan State University, East Lansing, Michigan, USA

[2]Department of Chemical Engineering and Materials Science, Michigan State University, East Lansing, Michigan, USA

[3]Department of Earth and Environmental Science, Michigan State University, East Lansing, Michigan, USA

[4]W. K. Kellogg Biological Station, Michigan State University, Hickory Corners, Michigan, USA

[5]Department of Plant, Soil and Microbial Sciences, Michigan State University, East Lansing, Michigan, USA

[6]Department of Chemical and Biological Engineering, Princeton University, Princeton, New Jersey, USA

[7]Andlinger Center for Energy and Environment, Princeton University, Princeton, New Jersey, USA

[8]DOE Great Lakes Bioenergy Research Center, University of Wisconsin-Madison, Madison, Wisconsin, USA

[9]Department of Entomology, Michigan State University, East Lansing, Michigan, USA

[10]Nelson Institute Center for Sustainability and the Global Environment (SAGE), University of Wisconsin-Madison, Madison, Wisconsin, USA

[11]Department of Plant, Soil and Microbial Sciences, Michigan State University, East Lansing, Michigan, USA

Correspondence
Seungdo Kim, DOE Great Lakes Bioenergy Research Center, Michigan State University, East Lansing, MI 48824, USA.
Email: kimseun@egr.msu.edu

Funding information
U.S. Department of Energy, Grant/Award Number: DE-SC0018409; USDA NIFA; Michigan State University

Abstract

Energy crops for biofuel production, especially switchgrass (*Panicum virgatum*), are of interest from a climate change perspective. Here, we use outputs from a crop growth model and life cycle assessment (LCA) to examine the global warming intensity (GWI; g CO_2 MJ^{-1}) and greenhouse gas (GHG) mitigation potential (Mg CO_2 $year^{-1}$) of biofuel systems based on a spatially explicit analysis of switchgrass grown on marginal land (abandoned former cropland) in Michigan, USA. We find that marginal lands in Michigan can annually produce over 0.57 hm^3 of liquid biofuel derived from nitrogen-fertilized switchgrass, mitigating 1.2–1.5 Tg of CO_2 $year^{-1}$. About 96% of these biofuels can meet the Renewable Fuel Standard (60% reduction in lifecycle GHG emissions compared with conventional gasoline; GWI ≤37.2 g CO_2 MJ^{-1}). Furthermore, 73%–75% of these biofuels are carbon-negative (GWI less than zero) due to enhanced soil organic carbon (SOC) sequestration. However, simulations indicate that SOC levels would fail to increase and even decrease on the 11% of lands where SOC stocks >>200 Mg C ha^{-1}, leading to carbon intensities greater than gasoline. Results highlight the strong climate mitigation potential of switchgrass grown on marginal lands as well as the needs

to avoid carbon rich soils such as histosols and wetlands and to ensure that productivity will be sufficient to provide net mitigation.

KEYWORDS

γ-valerolactone (GVL), cellulosic biofuel, dynamic LCA, global warming intensity, marginal land, static LCA, switchgrass

1 | INTRODUCTION

Maintaining a global temperature increase below 1.5°C relies significantly on the large scale deployment of negative CO_2 emissions (carbon dioxide removal) technologies (Fuss et al., 2018; Intergovernmental Panel on Climate Change, 2018; Minx et al., 2018; Nemet et al., 2018). Negative emission technologies particularly applicable to the cellulosic biofuel production system are soil organic carbon (SOC) sequestration and carbon capture and storage (CCS). Combining these two technologies can mitigate greenhouse gas (GHG) emissions more efficiently than can any single technology alone (Gelfand et al., 2020; Kim et al., 2020).

Marginal lands such as those abandoned from agriculture due to low soil fertility or other environmental factors (Emery et al., 2017; Gelfand et al., 2013; Khanna et al., 2021) can be attractive locations to grow bioenergy crops in order to minimize or avoid food-fuel conflicts, indirect land use change effects, and debilitating carbon debts (Robertson et al., 2017). Switchgrass (*Panicum virgatum* L.), a native perennial warm-season grass, is considered a promising feedstock for cellulosic biofuel production due to its high productivity, ability to grow on low fertility soils, low input requirements, and potential for SOC sequestration (Follett et al., 2012; Jin et al., 2019; Liebig et al., 2008; Martinez-Feria et al., 2022; McLaughlin & Kszos, 2005; Tilman et al., 2006; U.S. Department of Energy, 2016; Wright & Turhollow, 2010).

Soil organic carbon increase by switchgrass ranges from −0.6 to 4.3 Mg C ha^{-1} $year^{-1}$, depending on climate, soil properties, land use history and so on (Agostini et al., 2015; Dheri et al., 2022; Follett et al., 2012; Jin et al., 2019; Lee et al., 2007; Lemus & Lal, 2005; Liebig et al., 2008; Slessarev et al., 2020; Valdez et al., 2017). According to Liebig et al. (2008), switchgrass decreases SOC at two of ten experimental sites due to a significant decrease in soil bulk density near the surface depth, which contributes to decreased SOC, whereas switchgrass increases SOC at the remaining experimental sites. Dheri et al. (2022) show that switchgrass grown in Ohio could increase SOC in the 0–20 cm depth by 8.22 Mg C ha^{-1} within the first 8 years of their study. Switchgrass production on marginally productive croplands can also increase SOC by 0.9–1.3 Mg C ha^{-1} $year^{-1}$ for 0–30 cm depth and over 2 Mg C ha^{-1} $year^{-1}$ for the 0–150 cm depth (Follett et al., 2012; Jin et al., 2019). In addition, switchgrass has the potential to support increased biodiversity and resulting ecosystem services in agricultural landscapes (Werling et al., 2014). Biofuels derived from switchgrass can be carbon negative due to SOC sequestration during switchgrass production (Dwivedi et al., 2015; Schmer et al., 2014) or due to CCS during its biorefining (Gelfand et al., 2020).

Most bioenergy modeling efforts are implicitly based on a static approach, which is based on average (or time-independent) values for foreground and background systems (Adler et al., 2007; Dwivedi et al., 2015; Kim & Dale, 2015; Kim et al., 2019, 2020; Schmer et al., 2008, 2014; Tao, Tan, et al., 2014; Wang et al., 2012). Unlike static life cycle assessments (LCAs), dynamic LCAs use time-dependent values for the foreground system, dynamic inventory data, and dynamic characterization factors to reduce uncertainty (International Organization for Standardization, 2006). Dynamic LCAs in the bioenergy system can capture annual fluctuations in biomass yields and subsequent SOC changes due to weather, as well as changes in electricity fuel mixes that affect GHG avoidance benefits. Relatively few studies, however (Albers et al., 2020; Almeida et al., 2015; Daystar et al., 2017; Levasseur et al., 2010; Yang & Chen, 2014), have used dynamic modeling. Yang and Chen (2014) estimated time-dependent GHG emissions associated with electricity based on historical data in their crop residue gasification study. Levasseur et al. (2010) developed time-dependent dynamic global warming potentials (GWPs) for CO_2 and other GHGs based on the cumulative radiative forcing concept. Daystar et al. (2017) showed that dynamic GHG accounting is a more robust method than the static GHG accounting method because of temporal boundaries.

Here, we estimate the global warming intensity (GWI; g CO_2 MJ^{-1}) of biofuel produced from switchgrass grown on marginal lands in Michigan and its GHG mitigation potential (Mg CO_2 $year^{-1}$) with SOC changes and biomass yields estimated by the system approach to land use sustainability (SALUS) model (Basso & Ritchie, 2015). We use results to populate both a static (time-independent) and dynamic LCA to calculate GWI and GHG mitigation. The time-independent GWPs are considered under both

the static and dynamic approaches to compare with the GWI of gasoline (93.08 g CO_2 MJ^{-1}; U.S. Environmental Protection Agency, 2010), with a time horizon of 100 years.

2 | METHODS

2.1 | Area of study and marginal lands identification

We conducted this analysis for the state of Michigan USA (see Figure S1), which is in the northern portion of the US Corn Belt. The region has a humid continental climate (Köppen climate classification Dfb), with warm, short summers and cold, icy winters, and precipitation well distributed throughout the year. On average, the region receives 795 mm of annual precipitation, and the average daily temperature is 7.9°C (Liu & Basso, 2017). Land cover is dominated by cropland in the south, and deciduous and boreal woodlands in the north. Michigan also features a significant amount of lands that have been abandoned from annual crop production for varying periods (Lark et al., 2020), which means that such lands could be attractive for growing biomass crops because of their low opportunity cost (Kells & Swinton, 2014).

We identify marginal lands using land capability classes (LCC) as defined by the US Department of Agriculture in the SSURGO database (https://sdmdataaccess.sc.egov.usda.gov). Following Gelfand et al. (2013), we consider soils with LCCs I–IV to be productive agricultural land excluded from the analysis. From the remaining soils (LCCs V–VIII), we further exclude those classified as urban as well as carbon dense habitats such as forests and wetlands as identified in the Cropland Data Layer (Boryan et al., 2011).

2.2 | Crop growth modeling

We used the SALUS model to estimate the potential yield and SOC changes in the identified marginal land sites. SALUS is a biogeochemical cropping systems simulation platform that contains process-based models to simulate crop growth and development, and carbon, water, and nutrient cycling on a daily time step basis. Model inputs are daily values of incoming solar radiation ($MJ\,m^{-2}$), maximum and minimum air temperature (°C), and rainfall (mm), as well as information on soil characteristics and management. The SALUS model has been validated for several crops and management practices (Basso & Ritchie, 2015) and was previously used to spatially simulate switchgrass yields across Michigan (Liu & Basso, 2017) and to evaluate soil carbon sequestration from switchgrass across the US Midwest (Martinez-Feria & Basso, 2020). The SALUS switchgrass model has been validated under conditions of both loss and gains of SOC (Martinez-Feria & Basso, 2020). Martinez-Feria et al. (2022) used data from 28 experimental sites across eight Midwestern states to satisfactorily estimate observed yields and SOC change.

We used the SALUS model (Basso & Ritchie, 2015; Martinez-Feria & Basso, 2020) to simulate the yield of a switchgrass crop planted on marginal land following a conventional tillage event at 30 cm depth which allowed for the incorporation of the previous vegetation (mixed annual and perennial plants). The procedure of tilling and incorporating the previous vegetation was chosen to represent a realistic scenario. The large first-year losses of SOC from the conversion of marginal land to switchgrass is considered conservative rather than choosing a scenario with conditions which would produce results more favorable to growing bioenergy crops in terms of reduced SOC losses (e.g., no tillage).

For weather inputs we used the Gridded Surface Meteorological dataset (gridMET; http://www.climatologylab.org/gridmet.html; Abatzoglou, 2013), a high-resolution (~4 km, daily) weather dataset ideal for land surface modeling. For every 30 × 30 m grid point within our study area, we used daily weather values for the period of 1980–2019. Data on soil characteristics at every site are retrieved from the gridded SSURGO dataset (30 m resolution) and used to configure the soil component of the model following the methodology described by Liu and Basso (2017). The model is run for each 30 m grid cell for each combination of soil and weather inputs, resulting in 750,000 unique simulations.

We ran each simulation for 30 years and assumed each stand is replanted on each 11th year of the simulation following harvest and tillage events. This means that each simulation encompasses three planting cycles. To avoid confounding the effect of weather year and renewal of the perennial stand, the year to start the simulation for each grid cell was chosen at random from the first 10 years in the gridMET dataset (1980–1989). Plantings were simulated to occur in mid-May, and annual harvests in mid-October. The simulation considered both unfertilized (N0) and fertilized (N50) scenarios, with the fertilized scenarios receiving 50 kg N ha^{-1} top-dressed in late May every year. Based on evidence from long-term experiments in the region, we assume a 65% harvest efficiency, that is, that 35% of total above ground net primary productivity is returned to the soil as plant residues prior to or during harvest operations (Martinez-Feria & Basso, 2020). Outputs from the simulation are annual dry biomass yields ($Mg\,ha^{-1}$), hereafter referred to as switchgrass production, and annual SOC contents (Mg C ha^{-1}; 0–15, 15–40, 40–90 cm and entire soil profile). The grid cells are aggregated based

on proximity to ~40,000 individual parcels, considered as farm units supplying switchgrass to the biorefinery. The median size of individual parcels is 1.76 ha, and ranges from 0.01 to over 100 ha.

2.3 | Biofuel production system

We include in our analysis only those land parcels capable of producing one biomass bale (541 dry kg, Hess et al., 2009) at least 9 of 10 years to avoid excessive logistics costs. Baled switchgrass is assumed to be transported from these marginal land parcels to a centralized biorefinery by truck and then processed to produce biofuel.

The centralized biorefinery consists of facilities for feedstock handling, pretreatment (if applicable), enzyme production (if applicable), hydrolysis, fermentation, cogeneration and wastewater treatment. Biofuel yield from switchgrass is assumed to be equal to that from corn stover (Argonne National Laboratory, 2020). Two different hydrolysis technologies are considered in the analysis: (1) chemical hydrolysis and (2) enzymatic hydrolysis. The chemical hydrolysis technology uses a mixture of γ-valerolactone (GVL), water, and toluene plus dilute sulfuric acid as a catalyst to hydrolyze cellulose and hemicellulose into fermentable sugars (Won et al., 2017). In the enzymatic hydrolysis technology, dilute acid pretreatment is performed prior to the enzymatic hydrolysis (Tao, Schell, et al., 2014). Process data for the biorefinery are obtained from the literature: one process data set for the biorefinery with chemical hydrolysis technology (referred to as "CHEM", Won et al., 2017) and two process data sets for the biorefinery with enzymatic hydrolysis technology (referred to as "ACID", Tao, Schell, et al., 2014 and "GREET", Argonne National Laboratory, 2020, respectively). The assumptions and parameters relevant to the biorefinery are summarized in Tables S1 and S2.

2.4 | Static GHG emissions

The GWI of biofuel includes GHG emissions associated with switchgrass production, transportation of baled switchgrass to a biorefinery, storage, biorefinery operations, transportation/distribution of biofuel, avoided grid electricity, biofuel combustion, and upstream processes (e.g., materials and fuels). GHG emissions of switchgrass production per hectare on each marginal land parcel are calculated based on average values over 30 years. GHG emissions of switchgrass production derive from agronomic inputs (i.e., seed, fertilizers, and herbicides), fuel for field operations, CO_2 emissions from SOC change, and N_2O emissions. The agronomic inputs and fuel use are obtained from field experiment data at the Great Lakes Bioenergy Research Center (GLBRC) biofuel cropping system experimental site and marginal land experimental sites in Michigan (https://data.sustainability.glbrc.org/datatables). Although little phosphorus and potassium fertilizers have been applied in the two experimental sites, we conservatively assume that phosphorus and potassium fertilizers are applied annually at rates of 2 kg P_2O_5 and 7 kg K_2O dry Mg^{-1} of switchgrass harvested regardless of nitrogen application rate (U.S. Department of Energy, 2016). Fuel use per hectare is assumed to be constant regardless of the size of the marginal land parcel. CO_2 emissions from SOC change are calculated based on results from the SALUS simulations. N_2O emissions are estimated by the IPCC Tier 1 methodologies (Intergovernmental Panel on Climate Change, 2019). Both direct and indirect N_2O emissions are included in the calculations.

Average GHG emissions associated with one metric ton of switchgrass are estimated by dividing the average GHG emissions of switchgrass production per hectare by an average switchgrass yield. Since no biorefinery sites are specified in this analysis, the transport distance from marginal land parcels to a biorefinery is arbitrarily assumed to be 80.5 km (50 miles). GHG emissions associated with storage and transportation/distribution of biofuel are estimated using data from the literature (Argonne National Laboratory, 2020; Brownell, 2009). Surplus electricity from the biorefinery is exported to the grid and is assumed to displace the U.S. grid electricity. Biogenic CO_2 emissions from combusting biofuel are offset by carbon uptake of switchgrass and are not taken into account in these GHG calculations. Thus, the GHG emissions of combusting biofuel include only CH_4 and N_2O emissions from tailpipe combustion (U.S. Environmental Protection Agency, 2010).

The GHG emissions of materials and energy production are calculated based on the unit process data obtained from the US Life Cycle Inventory Database (https://www.nrel.gov/lci/), the Ecoinvent database version 3.4 (https://www.ecoinvent.org/database/database.html), and the GREET model (Argonne National Laboratory, 2020). Matrix inversion (Frischknecht et al., 2007) is used to calculate the cumulative GHG emissions associated with materials and energy productions. The GHG emissions associated with a product (or an energy flow) can be split into two categories: off-process and in-situ process (gate-to-gate) GHG emissions. The off-process emissions are the GHG emissions associated with other products (or energy) involved in the product system of interest (e.g., upstream and downstream processes—raw materials and input fuels production, transportation, waste management, etc.). The in-situ process emissions are the GHG emissions released from the unit process that generates

the product (or energy flow) of interest. Thus, the cumulative GHG emissions associated with the mth product, e_m, can be expressed as:

$$e_m = p_m + u_m, \tag{1}$$

where p_m is the in-situ process GHG emissions of the mth product production process, and u_m is the off-process GHG emissions of the mth product production process. The GHGs in this analysis include CO_2, CH_4 and N_2O. The off-process GHG emissions, u_m, can be calculated as

$$u_m = \sum a_{l,m} \cdot e_l, \tag{2a}$$

$$= \sum a_{l,m} \cdot (p_l + u_l), \tag{2b}$$

$$= \sum a_{l,m} \cdot p_l + \sum a_{l,m} \cdot u_l, \tag{2c}$$

where a is the economic entity defined by Heijungs (1994). For example, $a_{l,m}$ denotes the quantity of the lth product (or energy) involved in the mth product production process. The economic entity is obtained from the unit process data. Note that the economic entities for multi-functional processes in Equation (2a) are allocated entities via proper methods (e.g., physical or economic properties, etc.), which are provided by the databases. The GHG emissions of a product (an energy) can be written in a matrix form.

$$\mathbf{E} = \mathbf{P} + \mathbf{U}, \tag{3a}$$

$$\mathbf{U} = \mathbf{A} \cdot \mathbf{E}, \tag{3b}$$

$$\mathbf{U} = \mathbf{A} \cdot (\mathbf{P} + \mathbf{U}). \tag{3c}$$

Solving Equation (3c) if $\mathbf{A}$ is a nonsingular matrix, the off-process emission matrix, $\mathbf{U}$, is

$$\mathbf{U} = [\mathbf{I} - \mathbf{A}]^{-1} \cdot \mathbf{A} \cdot \mathbf{P}, \tag{4}$$

where $\mathbf{I}$ is the identity matrix. The cumulative GHG emissions, $\mathbf{E}$, therefore become

$$\mathbf{E} = \mathbf{P} + [\mathbf{I} - \mathbf{A}]^{-1} \cdot \mathbf{A} \cdot \mathbf{P}. \tag{5}$$

The 2016 electricity fuel mix (U.S. Energy Information Administration, 2018) is used to calculate the cumulative GHG emissions of materials and energy in the static approach. The transmission and distribution loss for electricity (4.5%; U.S. Environmental Protection Agency, 2018) is also included in the calculations. The cumulative GHG emissions for materials and energy are shown in Figure S2. GHG emissions associated with transportation of materials and energy (US Department of Transportation, 2015) are included in the cumulative GHG emissions.

Greenhouse gas mitigation by biofuel is categorized into two types: carbon removal and GHG avoidance. The carbon removal is the net sum of carbon absorbed by SOC sequestration and GHG emissions released from the biofuel system (including switchgrass production, transportation, storage, biorefinery, distribution and combustion). The GHG avoidance is avoided life cycle GHG emissions associated with alternative systems (i.e., grid electricity and gasoline) displaced by the biofuel system.

2.5 | Dynamic (time-dependent) approach

In the dynamic approach, annual GHG emissions of materials and fuels are projected based on the electricity fuel mixes from 2016 to 2045 (see Figure S3). No evolution of technologies (e.g., "technological advances", "technological shift", etc.) in the material and fuel productions are assumed in the dynamic approach due to lack of data. Two electricity fuel-mix projections are considered in the dynamic approach. The electricity fuel mix projections by the U.S. Energy Information Administration (2019) are used in the first projection (referred to as "P_EIA", see Figure S3a). The second projection ("P_COAL", see Figure S3b) assumes that after 2023 (arbitrarily chosen), fossil fuels except for natural gas decline faster than in the first projection, using maximum annual decrease rates in the first projection. In contrast to coal and petroleum, the projections for natural gas and nuclear in the second projection are the same as in the first projection. The differences are therefore assigned to renewable energy sources. As seen in Figure S3b, coal is projected to be totally phased out in 2035 in the second projection.

Greenhouse gas emissions of switchgrass production per hectare on each marginal land parcel for each year are calculated, and then are divided by switchgrass yield in a given year to calculate GHG emissions of one metric ton of switchgrass. When no switchgrass is harvested from a particular parcel in a given year, the GHG emissions of switchgrass production are assigned to the next harvest year. GHG emissions of agronomic inputs, fuels and materials used in the biofuel system during each year are calculated based on the electricity fuel mix of the harvest year through Equations (3–5). We assume that the GHG avoidance from the surplus electricity is calculated based on the electricity fuel mix of the year following harvest, implying that the surplus electricity from switchgrass-based biofuel system displaces electricity in the year following harvest. However, the GHG avoidance from the surplus

electricity is assigned to the switchgrass production year for consistency and ease of understanding. More information on methods and background data can be found in Kim et al. (2023).

3 | RESULTS

3.1 | GHG emissions of switchgrass in the static approach

The total potentially available marginal land in Michigan is 324,000 ha. However, not all of these lands are suitable for biofuel production: The GWI of biofuels derived from switchgrass grown on about 11% of available marginal lands (35–36,000 ha) is greater than that of gasoline due to high SOC loss (see Figures S5 and S7). We thus exclude these lands from further analysis, leaving 288,000 ha available for further analysis. Results from the SALUS model show that switchgrass yield with no nitrogen fertilizer added (0N) is 30% lower on average compared to 50N (see Figure S6), very close to field experiment results from the GLBRC marginal land experimental sites in Michigan (https://data.sustainability.glbrc.org/datatables). Mean switchgrass yield is 5.35 (±2.18) Mg ha^{-1} year^{-1} for 0N and 7.65 (±2.87) Mg ha^{-1} year^{-1} for 50N, and the total annual switchgrass production is 1.5 Tg of biomass for 0N and 2.2 Tg of biomass for 50N.

The area-weighted simulated average SOC sequestration rates are 0.09 (±0.14) and 0.39 (±0.23) Mg C ha^{-1} year^{-1} for 0N and 50N, respectively. However, switchgrass production and harvesting on about 22% of the marginal land of 288,000 ha for a fertilizer application rate of 0N and on about 6% of 288,000 ha for an application rate of 50N reduces SOC levels by 0.13 (±0.14) and 0.19 (±0.18) Mg C ha^{-1} year^{-1}, respectively (see Figure S7). Results from the SALUS model show that switchgrass production on marginal lands with low initial SOC stock increases SOC levels. In contrast, switchgrass production on marginal lands with high initial SOC stocks (>200 Mg C ha^{-1}) reduces SOC regardless of the nitrogen fertilizer application (see Figure S8). Several field studies (Goidts et al., 2009; Kampf et al., 2016; Mann, 1986; Minasny et al., 2017; Saby et al., 2008; Sollins et al., 1996; Zhao et al., 2013) also show that soils with low initial SOC stock increased SOC, but soils with high initial SOC stock lose SOC.

Mass-weighted average GHG emissions of switchgrass grown on suitable marginal lands in Michigan are 15.3 (±99.6) kg CO_2 Mg^{-1} for 0N and −62.8 (±117.1) kg CO_2 Mg^{-1} for 50N. Approximately 60% of unfertilized switchgrass grown on marginal lands (0.9 Tg of biomass) has negative GHG emissions (see Figure S10) and can remove 0.11 Tg of CO_2 year^{-1} directly from the atmosphere and sequester the atmospheric carbon in soil, resulting in net GHG mitigation of 0.05 Tg of CO_2 year^{-1}. About 76% of fertilized switchgrass (1.7 Tg of switchgrass biomass) has negative GHG emissions (see Figure S10) and can sequester 0.41 Tg of atmospheric CO_2 year^{-1} in soil. The net GHG mitigation by fertilized switchgrass with negative GHG emissions amounts to 0.20 Tg of CO_2 year^{-1}. SOC sequestration is the major source of negative emissions, and the mass-weighted average SOC sequestration is 58.9 (±96.4) kg CO_2 Mg^{-1} for 0N and 188.1 (±113.9) kg CO_2 Mg^{-1} for 50N (see Figure 1). N_2O emissions from fertilized switchgrass are greater than those from unfertilized switchgrass production because of N_2O resulting from nitrogen fertilizer application.

3.2 | GWI in the static approach

The total annual biofuel production on the suitable marginal lands in Michigan is 0.40–0.49 hm^3 for 0N and 0.57–0.71 hm^3 for 50N, depending on the biorefinery model

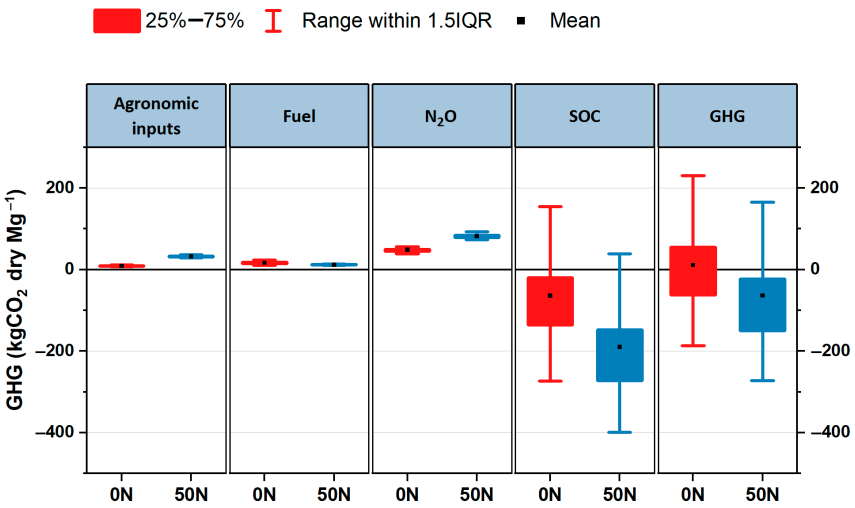

FIGURE 1 Breakdown of GHG emissions of switchgrass in the static approach. "Agronomic inputs" include GHG emissions of fertilizers (N, P, K), seed and herbicides. "Fuel" is GHG emissions associated with diesel used in field operations. "SOC" is GHG emissions of SOC sequestration. "N_2O" is N_2O emissions. GHG, greenhouse gas; IQR, interquartile range; SOC, soil organic carbon

employed. Volume-weighted average GWI of biofuel derived from unfertilized switchgrass (0N) is from 5.0 to 7.6 g CO_2 MJ^{-1}, while volume-weighted average GWI of biofuel derived from fertilized switchgrass (50N) is negative, ranging from −9.4 to −4.8 g CO_2 MJ^{-1} (see Table 1). More than 93% of biofuels derived from switchgrass grown on marginal lands (equivalent to 85%–87% of the total available marginal lands) meet the 60% GHG reduction requirement of the U.S. Energy Independence and Security Act (U.S. Environmental Protection Agency, 2010), regardless of nitrogen fertilizer application. About 41%–51% of biofuels derived from unfertilized switchgrass (0.17–0.20 hm^3 $year^{-1}$) and 73%–75% of biofuels derived from fertilized switchgrass (0.43–0.52 hm^3 $year^{-1}$) are carbon negative (see Figures S11–S13).

Marginal lands for switchgrass production resulting in carbon-negative biofuels have low initial carbon stock (See Figures S14–S16). The initial carbon stock in over 70% of Michigan marginal lands for switchgrass production for carbon-negative biofuels is less than 100 Mg C ha^{-1}. The initial SOC stock could be one of the key indicators of (spatially) differentiated GWI. As seen in Figures S17–S19, the GWI of biofuels derived from switchgrass grown on marginal lands tends to increase with initial SOC stock due to large SOC losses in carbon-rich marginal lands. The GHG tradeoff between SOC loss and biomass yield is insignificant. Carbon-rich soils can achieve high biomass yield (see Figure S9), but GHG emissions from SOC loss are so large that the positive effect of high biomass yield is negligible.

The CHEM model (biorefinery with chemical hydrolysis technology) has the lowest average GWI among other models regardless of nitrogen fertilizer application. The primary reason that the CHEM model achieved the lowest average GWI is that it provides the greatest GHG avoidance from the surplus electricity compared to the other models (−25 g CO_2 MJ^{-1}). The GHG avoided by the surplus electricity is −19 g CO_2 MJ^{-1} for the ACID model and −17 g CO_2 MJ^{-1} for the GREET model. Volume-weighted average GHG emissions associated with unfertilized switchgrass in the GWI of biofuel are from 2.7 to 2.8 g CO_2 MJ^{-1}, while volume-weighted average GHG emissions of fertilized switchgrass range from −11.5 to −9.0 g CO_2 MJ^{-1}, depending on the biorefinery models, especially as these models determine biofuel yields (see Figures S20–S22). GHG emissions associated with the biorefinery are 16–18 g CO_2 MJ^{-1}.

TABLE 1 Biofuel volume and volume-weighted average global warming intensity (GWI) of biofuel derived from switchgrass grown on marginal lands

	Biofuel (hm^3 $year^{-1}$)		Static GWI (g CO_2 MJ^{-1})	
	0N	50N	0N	50N
CHEM	0.40	0.57	5.0 (±18.2)	−9.4 (±21.5)
ACID	0.41	0.59	7.6 (±17.6)	−6.2 (±20.8)
GREET	0.49	0.71	6.8 (±15.6)	−4.8 (±18.1)

3.3 | GHG mitigation in the static approach

The total GHG emissions from the biofuel production system based on switchgrass grown on marginal lands in Michigan (including CO_2 released from SOC loss, N_2O, GHG emissions of materials and fuels, etc., not including GHG avoidance from the surplus electricity) are 0.33–0.37 Tg CO_2 $year^{-1}$ for 0N and 0.56–0.61 Tg CO_2 $year^{-1}$ for 50N. Over 37% of the total GHG emissions in the biofuel production system come from biorefinery processes (see Figure S23).

In the biofuel production system based on fertilized switchgrass, GHG emissions from agronomic inputs and N_2O emissions account for 41%–45% of the total GHG emissions released, while in the biofuel production system based on unfertilized switchgrass, these emissions only account for 24%–27% of total GHG emissions. CO_2 released from SOC loss contributes 2%–9% of the total GHG emissions released. As mentioned previously, switchgrass production on some marginal lands (22% for unfertilized switchgrass production and 6% for fertilized switchgrass production) reduces the SOC level, thereby releasing CO_2 to the atmosphere. SOC sequestration is 0.12 Tg CO_2 $year^{-1}$ for the biofuel system based on unfertilized switchgrass and 0.43 Tg CO_2 $year^{-1}$ for the biofuel system based on fertilized switchgrass.

Greenhouse gas avoidance by displacing grid electricity ranges from 0.16 to 0.26 Tg CO_2 $year^{-1}$, and the GHG avoidance by displacing gasoline range between about 0.79 and 1.40 Tg CO_2 $year^{-1}$. The net GHG mitigation by biofuel is therefore 0.74–0.91 Tg CO_2 $year^{-1}$ for the biofuel system based on unfertilized switchgrass and 1.24–1.47 Tg CO_2 $year^{-1}$ for the biofuel system based on fertilized switchgrass (see Figure 2). Applying nitrogen fertilizer can increase the GHG mitigation by biofuel due to larger biofuel volume produced and lower GWI. The biofuel system based on the GREET model exhibits the greatest GHG mitigation regardless of nitrogen fertilizer application simply because of greater biofuel yield.

3.4 | Dynamic approach

We analyzed with the dynamic approach only the 50N case with the chemical hydrolysis technology. As seen

in Figure 3 (also Table S3), the dynamic GWIs in each year range from −415 to 442 g CO_2 MJ^{-1}, reflecting GHG emissions associated with each year's activities in the biofuel production system (e.g., switchgrass production, biorefinery, combustion, etc.), with a volume-weighted average of −7.2 (±21.4) g CO_2 MJ^{-1} in the P_EIA projection and of −3.0 (±21.4) g CO_2 MJ^{-1} in the P_COAL projection. The average dynamic GWI is higher than the average static GWI (−9.4 (±21.5) g CO_2 MJ^{-1}). The decline of coal used in the electricity fuel mix plays a major role in increasing GWI in the dynamic approach and reduces the GHG avoidance due to supplying surplus electricity to the grid by 12% and 35% in the P_EIA and the P_COAL projections, respectively. Changes in the electricity fuel mix reduce GHG emissions of materials and fuels by only 1%–3%. The GWI in the first year is much higher than GWIs in other years because of GHG emissions from CO_2 released from SOC loss. The SOC sequestration rates in the first 3 years are negative (see Figures S24 and S25), −0.87 (±0.77) Mg C ha^{-1} $year^{-1}$ for the first year, −0.40 (±0.61) Mg C ha^{-1} $year^{-1}$ for the second year and −0.20 (±0.46) Mg C ha^{-1} $year^{-1}$ for the third year. After the third year, SOC sequestration rates become positive.

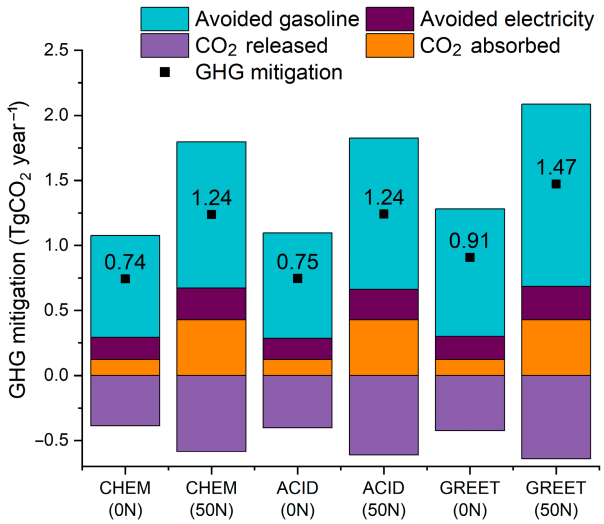

FIGURE 2 GHG mitigation for 288,000 ha of marginal land in Michigan for biofuel production using the static approach. CO_2 released includes GHG emissions of materials and fuels, CO_2 released from SOC loss and N_2O. CO_2 absorbed is atmospheric carbon absorbed by SOC sequestration. Avoided electricity is the GHG avoidance from the surplus electricity. Avoided gasoline is the GHG avoidance by displacing gasoline. GHG, greenhouse gas; SOC, soil organic carbon

As seen in the dynamic GWI pattern in Figure 3, the GWIs in the final year of any planting cycle (11th and 22nd years) rapidly decline compared to the GWI in the previous year. The primary reason for the rapid GWI declines is dead biomass at the end of the cycle, which is incorporated into the soil and increases SOC level, resulting in a high SOC sequestration rate, particularly SOC sequestration rate at a soil depth of 15 cm (see Figures S24 and S25). The GWIs in the establishment year of the second and third planting cycles (12th and 23rd years) decline more rapidly and are much lower than those in other years, less than −310 g CO_2 MJ^{-1} due to higher SOC sequestration rates and lower switchgrass yields in the establishment year (see Figures S24 and S25). The SOC sequestration rates in the second and third years after planting switchgrass (except for the first planting cycle) decrease compared to the SOC sequestration rate in the establishment year; hence GWIs increase greatly in those 2 years. After the third year, GWIs are relatively stable until the final year of a given planting cycle.

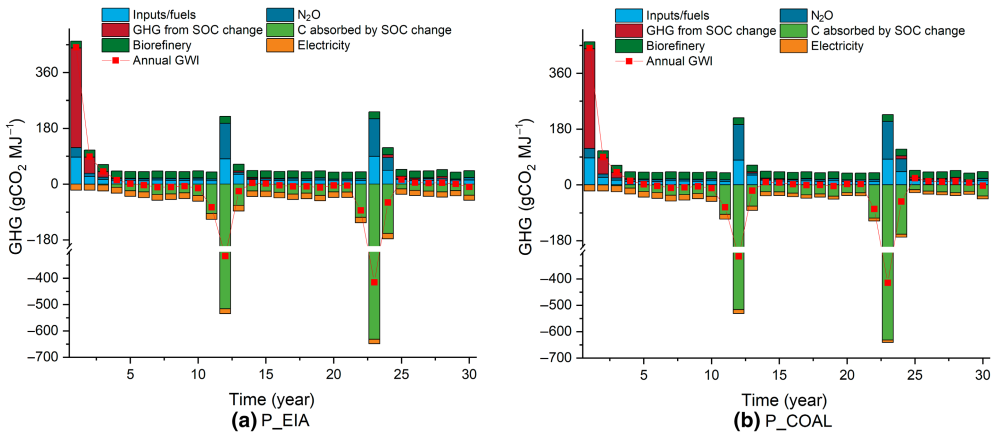

FIGURE 3 GWI in the dynamic approach. "Inputs/fuels" includes GHG emissions of fertilizers (N, P, K), seed, herbicides and fuels. "N_2O" is N_2O emissions. "GHG from SOC change" is GHG emissions from SOC loss. "C absorbed by SOC change" is atmospheric carbon absorbed by SOC sequestration. "Electricity" is GHG avoidance from the surplus electricity. "Biorefinery" is GHG emissions of biorefinery, transportation, storage, distribution and combustion. GHG, greenhouse gas; GWI, global warming intensity; SOC, soil organic carbon

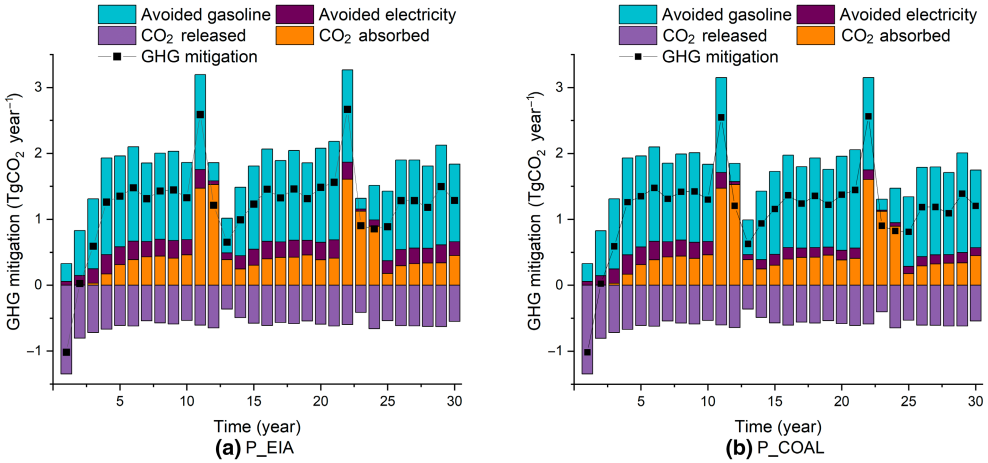

FIGURE 4 GHG mitigation in the dynamic approach. CO_2 released includes GHG emissions of materials and fuels, CO_2 released from SOC loss and N_2O. CO_2 absorbed is atmospheric carbon absorbed by SOC sequestration. Avoided electricity is the GHG avoidance from the surplus electricity. Avoided gasoline is the GHG avoidance by displacing gasoline. GHG, greenhouse gas; SOC, soil organic carbon

As seen in the spatial and temporal GWIs for each parcel (see Figures S26 and S27), the GWIs of some parcels are significantly higher than those of other parcels in most years (except the final year of each planting cycle). Higher GWIs in those parcels are caused by lower SOC sequestration rates in those years compared to SOC sequestration rates in other parcels. Due to low SOC sequestration rates and higher N_2O emissions, the GWIs of approximately 42% of total parcels in Wayne County (southeast Michigan) in the establishment year of the second and third planting cycles (12th and 23rd years) are greater than the GWI of gasoline.

In the first year after converting marginal lands to switchgrass production, GHGs released from the biofuel production system are much larger than the sum of carbon absorbed and GHG avoidances due to SOC loss; hence about 1.1 Tg of CO_2 is released (see Figure 4). After the first year, biofuel derived from switchgrass can mitigate GHG emissions by between 0.03–2.6 Tg CO_2 year^{-1}. The biofuel volume in the establishment year of the second and third planting cycles is 12%–20% lower than the biofuel volume in the final year of the previous planting cycle, resulting in less GHG avoidance (see Figure 4).

4 | DISCUSSION

Biofuel volume produced annually varied greatly across the study region. Based on switchgrass availability, Northern Michigan, and northern regions of Central and Western Michigan are likely the best candidate locations for a biorefinery when switchgrass grown on marginal lands is the sole feedstock for biofuel production (see Figure S28). Approximately 74% of switchgrass grown on marginal lands in Michigan could be transported to a biorefinery less than 137 km distant (see Figure S29), and from a logistics perspective, a bale-based logistics system would be preferred.

In contrast, a pellet-based logistics system is favored for about 26% of switchgrass grown in Michigan. Considering the cost of pelletization and transportation, the break-even distance between bale- and pellet-based logistics systems is about 137 km (Sokhansanj et al., 2010). Most of switchgrass produced in the upper peninsula of Michigan would be transported over 137 km, and a depot (pellet)-based biorefinery system would be needed for biofuel production from switchgrass.

Chen et al. (2021) used the DayCent biogeochemical model to estimate the GWI of biofuel derived from switchgrass grown on Conservation Reserve Program (CRP) land in the eastern United States and found that the GWI of switchgrass-based biofuel is 1.69 g CO_2 MJ^{-1}, which is slightly higher than the GWIs in this study (see Table S4). The main difference between two studies is the change in SOC caused by biofuel yield, climate, biogeochemical model, time horizon (30-year vs. 14-year), simulation resolution (30 × 30 m vs. county), spatial boundary (Michigan vs. eastern region of the U.S.), and so on. However, both studies show that switchgrass production can raise SOC level.

The differences in the total GHG mitigation by biofuel between the static and dynamic approaches are small: only 2%–6%. GHG avoidance from the surplus electricity, which depends greatly on the electricity fuel mix, especially the fraction of coal in the mix, plays a major role in the differences between two approaches. The dynamic approach clearly reflects the effect of annual biomass yield fluctuations and the effect of future changes in the electricity fuel mix on GWI and GHG mitigation by biofuel. Therefore, the dynamic approach would be more

appropriate for the biofuel production system. However, results from the static approach are also important from a legislative and policy point of view because they are less uncertain.

The dynamic approach used in this study is incompletely realized, and there is room for improvement such as by utilizing or developing full dynamic inventory data (including "technological advances", "technological shift", etc.), time-dependent characterization factors, and so on (Levasseur et al., 2010; Lueddeckens et al., 2020; Sohn et al., 2020). Evolution of technologies would be forecasted by expert surveys, policies, extrapolation from historical data, discount rate method, and other methods (Lueddeckens et al., 2020; Tiruta-Barna et al., 2016; Yuan et al., 2015). Since modeling full dynamic inventory data is time-consuming (Beloin-Saint-Pierre et al., 2017; Hu, 2018), major GHG source processes in the biofuel production system (e.g., grid electricity, biorefinery, fertilizers, etc.) would be the best candidates for building dynamic inventory data.

As they are defined in our study, marginal lands clearly can produce crops for biofuel production to mitigate GHG emissions. This finding is consistent with the existing literature and suggests carbon-negative biofuels derived from switchgrass grown on marginal land could contribute to keeping the global temperature increase below 1.5°C (Intergovernmental Panel on Climate Change, 2018; Robertson et al., 2022). Furthermore, concentrating this energy crop production on marginal lands can reduce potential food-versus-fuel conflicts, further improving the environmental and societal benefits of such systems.

However, not all marginal lands are suitable for biofuel production. In Michigan, the GWI of biofuel derived from switchgrass grown on about 11% of the total available marginal lands is greater than that of gasoline due to high SOC loss. The initial carbon stock in those 11% of marginal lands is very high (>>200 Mg C ha^{-1}) compared to marginal lands with negative GWI (see Figures S14–S16). This strongly implies that marginal lands with low initial SOC stock would be more favorable for producing switchgrass than carbon-rich lands. This result highlights the importance of site-specific assessment and using soil data, modeling, and other means to determine site-specific suitability of marginal lands for biofuel production prior to planting energy crops on such lands.

ACKNOWLEDGMENTS

This article is based upon work supported by the US Department of Energy, Office of Science, Office of Biological and Environmental Research (DE-SC0018409), USDA NIFA, and Michigan State University AgBioResearch program.

CONFLICT OF INTEREST

The authors declare no conflict of interest.

DATA AVAILABILITY STATEMENT

Background information (SALUS simulation results, LCIs, electricity fuel mixes, and equation) is available in Dryad (https://doi.org/10.5061/dryad.wpzgmsbq8).

ORCID

Seungdo Kim https://orcid.org/0000-0001-9450-0249
Rafael Martinez-Feria https://orcid.org/0000-0002-4230-5684
Bruno Basso https://orcid.org/0000-0003-2090-4616
G. Philip Robertson https://orcid.org/0000-0001-9771-9895

REFERENCES

Abatzoglou, J. T. (2013). Development of gridded surface meteorological data for ecological applications and modelling. *International Journal of Climatology*, *33*(1), 121–131. https://doi.org/10.1002/joc.3413

Adler, P. R., Del Grosso, S. J., & Parton, W. J. (2007). Life-cycle assessment of net greenhouse-gas flux for bioenergy cropping systems. *Ecological Applications*, *17*(3), 675–691. https://doi.org/10.1890/05-2018

Agostini, F., Gregory, A. S., & Richter, G. M. (2015). Carbon sequestration by perennial energy crops: Is the jury still out? *Bioenergy Research*, *8*, 1057–1080. https://doi.org/10.1007/s12155-014-9571-0

Albers, A., Avadi, A., Benoist, A., Collet, P., & Helias, A. (2020). Modelling dynamic soil organic carbon flows of annual and perennial energy crops to inform energy-transport policy scenarios in France. *Science of the Total Environment*, *718*, 135278. https://doi.org/10.1016/j.scitotenv.2019.135278

Almeida, J., Degerickx, J., Achten, W. M. J., & Muys, B. (2015). Greenhouse gas emission timing in life cycle assessment and the global warming potential of perennial energy crops. *Carbon Management*, *6*(5–6), 185–195. https://doi.org/10.1080/17583004.2015.1109179

Argonne National Laboratory. (2020). *The greenhouse gases, regulated emissions, and energy use in transportation model*. https://greet.es.anl.gov/

Basso, B., & Ritchie, J. T. (2015). Simulating crop growth and biogeochemical fluxes in response to land management using the SALUS model. In S. K. Hamilton, J. E. Doll, & G. P. Robertson (Eds.), *The ecology of agricultural landscapes: Long-term research on the path to sustainability* (pp. 252–274). Oxford University Press.

Beloin-Saint-Pierre, D., Levasseur, A., Margni, M., & Blanc, I. (2017). Implementing a dynamic life cycle assessment methodology with a case study on domestic hot water production. *Journal of Industrial Ecology*, *21*, 1128–1138.

Boryan, C., Yang, Z., Mueller, R., & Craig, M. (2011). Monitoring US agriculture: The US Department of Agriculture, National Agricultural Statistics Service. *Cropland Data Layer Program. Geocarto International*, *26*(5), 341–358. https://doi.org/10.1080/10106049.2011.562309

Brownell, D. K. (2009). *Analysis of biomass harvest, handling, and computer modeling* (Master thesis). The Pennsylvania State University.

Chen, L., Blanc-Betes, E., Hudiburg, T. W., Hellerstein, D., Wallander, S., DeLucia, E. H., & Khanna, M. (2021). Assessing the returns to land and greenhouse gas savings from producing energy crops on conservation reserve program land. *Environmental Science & Technology*, *55*(2), 1301–1309.

Daystar, J., Venditti, R., & Kelley, S. S. (2017). Dynamic greenhouse gas accounting for cellulosic biofuels: Implications of time based methodology decisions. *International Journal of Life Cycle Assessment*, *22*(5), 812–826. https://doi.org/10.1007/s11367-016-1184-8

Dheri, G. S., Lal, R., & Moonilall, N. I. (2022). Soil carbon stocks and water stable aggregates under annual and perennial biofuel crops in Central Ohio. *Agriculture Ecosystems & Environment*, *324*, 107715.

Dwivedi, P., Wang, W., Hudiburg, T., Jaiswal, D., Parton, W., Long, S., DeLucia, E., & Khanna, M. (2015). Cost of abating greenhouse gas emissions with cellulosic ethanol. *Environmental Science & Technology*, *49*(4), 2512–2522. https://doi.org/10.1021/es5052588

Emery, I., Mueller, S., Qin, Z., & Dunn, J. B. (2017). Evaluating the potential of marginal land for cellulosic feedstock production and carbon sequestration in the United States. *Environmental Science & Technology*, *51*(1), 733–741. https://doi.org/10.1021/acs.est.6b04189

Follett, R. F., Vogel, K. P., Varvel, G. E., Mitchell, R. B., & Kimble, J. (2012). Soil carbon sequestration by switchgrass and no-till maize grown for bioenergy. *Bioenergy Research*, *5*(4), 866–875. https://doi.org/10.1007/s12155-012-9198-y

Frischknecht, R., Jungbluth, N., Althaus, H. J., Doka, G., Dones, R., Hischier, R., Hellweg, S., Nemecek, T., Rebitzer, G., & Spielmann, M. (2007). *Overview and methodology. Final report ecoinvent data v2.0, No. 1*. Swiss Centre for Life Cycle Inventories.

Fuss, S., Lamb, W. F., Callaghan, M. W., Hilaire, J., Creutzig, F., Amann, T., Beringer, T., de Oliveira Garcia, W., Hartmann, J., Khanna, T., Luderer, G., Nemet, G. F., Rogelj, J., Smith, P., Vicente Vicente, J., Wilcox, J., del Mar Zamora Dominguez, M., & Minx, J. C. (2018). Negative emissions-part 2: Costs, potentials and side effects. *Environmental Research Letters*, *13*(6). https://doi.org/10.1088/1748-9326/aabf9f

Gelfand, I., Hamilton, S. K., Kravchenko, A. N., Jackson, R. D., Thelen, K. D., & Robertson, G. P. (2020). Empirical evidence for the potential climate benefits of decarbonizing light vehicle transport in the U.S. with bioenergy from purpose-grown biomass with and without BECCS. *Environmental Science & Technology*, *54*(5), 2961–2974. https://doi.org/10.1021/acs.est.9b07019

Gelfand, I., Sahajpal, R., Zhang, X., Izaurralde, R. C., Gross, K. L., & Robertson, G. P. (2013). Sustainable bioenergy production from marginal lands in the US Midwest. *Nature*, *493*(7433), 514–517. https://doi.org/10.1038/nature11811

Goidts, E., Wesemael, B. V., & Van Oost, K. (2009). Driving forces of soil organic carbon evolution at the landscape and regional scale using data from a stratified soil monitoring. *Global Change Biology*, *15*(12), 2981–3000. https://doi.org/10.1111/j.1365-2486.2009.01940.x

Heijungs, R. (1994). A generic method for the identification of options for cleaner products. *Ecological Economics*, *10*(1), 69–81. https://doi.org/10.1016/0921-8009(94)90038-8

Hess, J. R., Kenney, K. L., Ovard, L. P., Searcy, E. M., & Wright, C. T. (2009). *Commodity-scale production of an infrastructure-compatible bulk solid from herbaceous lignocellulosic biomass, INL/EXT-09-17527*. Idaho National Laboratory. https://bioenergy.inl.gov/Reports/Uniform%20Format%20Bioenergy%20Feedstock.pdf

Hu, M. (2018). Dynamic life cycle assessment integrating value choice and temporal factors—A case study of an elementary school. *Energy and Buildings*, *158*, 1087–1096.

Intergovernmental Panel on Climate Change. (2018). *Global warming of 1.5°C*. https://www.ipcc.ch/site/assets/uploads/sites/2/2019/06/SR15_Full_Report_Low_Res.pdf

Intergovernmental Panel on Climate Change. (2019). *2019 Refinement to the 2006 IPCC guidelines for National Greenhouse Gas Inventories*. https://www.ipcc.ch/report/2019-refinement-to-the-2006-ipcc-guidelines-for-national-greenhouse-gas-inventories/

International Organization for Standardization. (2006). *ISO 14040: Environmental management—Life cycle assessment—Principles and framework*.

Jin, V. L., Schmer, M. R., Stewart, C. E., Mitchell, R. B., Williams, C. O., Wienhold, B. J., Varvel, G. E., Follett, R. F., Kimble, J., & Vogel, K. P. (2019). Management controls the net greenhouse gas outcomes of growing bioenergy feedstocks on marginally productive croplands. *Science Advances*, *5*(12), eaav9318. https://doi.org/10.1126/sciadv.aav9318

Kampf, I., Holzel, N., Storrle, M., Broll, G., & Kiehl, K. (2016). Potential of temperate agricultural soils for carbon sequestration: A meta-analysis of land-use effects. *Science of the Total Environment*, *566*, 428–435. https://doi.org/10.1016/j.scitotenv.2016.05.067

Kells, B. J., & Swinton, S. M. (2014). Profitability of cellulosic biomass production in the Northern Great Lakes region. *Agronomy Journal*, *106*(2), 397–406. https://doi.org/10.2134/agronj2013.0397

Khanna, M., Chen, L., Basso, B., Cai, X., Field, J. L., Guan, K., Jiang, C., Lark, T. J., Richard, T. L., Spawn-Lee, S. A., Yang, P., & Zipp, K. Y. (2021). Redefining marginal land for bioenergy crop production. *GCB Bioenergy*, *13*, 1590–1609. https://doi.org/10.1111/gcbb.12877Madhu

Kim, S., & Dale, B. E. (2015). All biomass is local: The cost, volume produced, and global warming impact of cellulosic biofuels depend strongly on logistics and local conditions. *Biofuels Bioproducts & Biorefining-Biofpr*, *9*(4), 422–434. https://doi.org/10.1002/bbb.1554

Kim, S., Dale, B. E., Jin, M., Thelen, K. D., Zhang, X., Meier, P., Reddy, A. D., Jones, C. D., Cesar Izaurralde, R., Balan, V., Runge, T., & Sharara, M. (2019). Integration in a depot-based decentralized biorefinery system: Corn Stover-based cellulosic biofuel. *Global Change Biology Bioenergy*, *11*(7), 871–882. https://doi.org/10.1111/gcbb.12613

Kim, S., Dale, B. E., Martinez-Feria, R., Basso, B., Thelen, K., Maravelias, C. T., Landis, D., Lark, T., & Robertson, G. P. (2023). Data from: Global warming intensity of biofuel derived from switchgrass grown on marginal land in Michigan. *Dryad, Dataset*. https://doi.org/10.5061/dryad.wpzgmsbq8

Kim, S., Zhang, X., Reddy, A. D., Dale, B. E., Thelen, K. D., Jones, C. D., Cesar Izaurralde, R., Runge, T., & Maravelias, C. (2020). Carbon-negative biofuel production. *Environmental Science & Technology*, *54*(17), 10797–10807. https://doi.org/10.1021/acs.est.0c01097

Lark, T. J., Spawn, S. A., Bougie, M., & Gibbs, H. K. (2020). Cropland expansion in the United States produces marginal yields at high costs to wildlife. *Nature Communications*, *11*(1), 4295. https://doi.org/10.1038/s41467-020-18045-z

Lee, D. K., Owens, V. N., & Doolittle, J. J. (2007). Switchgrass and soil carbon sequestration response to ammonium nitrate, manure, and harvest frequency on conservation reserve program land. *Agronomy Journal*, *99*, 462–468. https://doi.org/10.2134/agronj2006.0152

Lemus, R., & Lal, R. (2005). Bioenergy crops and carbon sequestration. *Critical Reviews in Plant Sciences*, *24*(1), 1–21. https://doi.org/10.1080/07352680590910393

Levasseur, A., Lesage, P., Margni, M., Deschenes, L., & Samson, R. (2010). Considering time in LCA: Dynamic LCA and its application to global warming impact assessments. *Environmental Science & Technology*, *44*(8), 3169–3174. https://doi.org/10.1021/es9030003

Liebig, M. A., Schmer, M. R., Vogel, K. P., & Mitchell, R. B. (2008). Soil carbon storage by switchgrass grown for bioenergy. *Bioenergy Research*, *1*(3–4), 215–222. https://doi.org/10.1007/s12155-008-9019-5

Liu, L., & Basso, B. (2017). Spatial evaluation of switchgrass productivity under historical and future climate scenarios in Michigan. *GCB Bioenergy*, *9*(8), 1320–1332. https://doi.org/10.1111/gcbb.12417

Lueddeckens, S., Saling, P., & Guenther, E. (2020). Temporal issues in life cycle assessment—A systematic review. *International Journal of Life Cycle Assessment*, *25*(8), 1385–1401. https://doi.org/10.1007/s11367-020-01757-1

Mann, L. K. (1986). Changes in soil carbon storage after cultivation. *Soil Science*, *142*(5), 279–288. https://doi.org/10.1097/00010694-198611000-00006

Martinez-Feria, R., & Basso, B. (2020). Predicting soil carbon changes in switchgrass grown on marginal lands under climate change and adaptation strategies. *GCB Bioenergy*, *12*(9), 742–755. https://doi.org/10.1111/gcbb.12726

Martinez-Feria, R., Basso, B., & Kim, S. (2022). Boosting climate change mitigation potential of perennial lignocellulosic crops grown on marginal lands. *Environmental Research Letters*, *17*, 044004.

McLaughlin, S. B., & Kszos, L. A. (2005). Development of switchgrass (*Panicum virgatum*) as a bioenergy feedstock in the United States. *Biomass & Bioenergy*, *28*(6), 515–535. https://doi.org/10.1016/j.biombioe.2004.05.006

Minasny, B., Malone, B. P., McBratney, A. B., Angers, D. A., Arrouays, D., Chambers, A., Chaplot, V., Chen, Z., Cheng, K., Das, B. S., Field, D. J., Gimona, A., Hedley, C. B., Hong, S. Y., Mandal, B., Marchant, B. P., Martin, M., McConkey, B. G., Mulder, V. L., ... Winowiecki, L. (2017). Soil carbon 4 per mille. *Geoderma*, *292*, 59–86. https://doi.org/10.1016/j.geoderma.2017.01.002

Minx, J. C., Lamb, W. F., Callaghan, M. W., Fuss, S., Hilaire, J., Creutzig, F., Amann, T., Beringer, T., de Oliveira Garcia, W., Hartmann, J., Khanna, T., Lenzi, D., Luderer, G., Nemet, G. F., Rogelj, J., Smith, P., Vicente Vicente, J., Wilcox, J., & del Mar Zamora Dominguez, M. (2018). Negative emissions-part 1: Research landscape and synthesis. *Environmental Research Letters*, *13*(6). https://doi.org/10.1088/1748-9326/aabf9b

Nemet, G. F., Callaghan, M. W., Creutzig, F., Fuss, S., Hartmann, J., Hilaire, J., Lamb, W. F., Minx, J. C., Rogers, S., & Smith, P. (2018). Negative emissions-part 3: Innovation and upscaling. *Environmental Research Letters*, *13*(6). https://doi.org/10.1088/1748-9326/aabff4

Robertson, G. P., Hamilton, S. K., Barham, B. L., Dale, B. E., Izaurralde, R. C., Jackson, R. D., Landis, D. A., Swinton, S. M., Thelen, K. D., & Tiedje, J. M. (2017). Cellulosic biofuel contributions to a sustainable energy future: Choices and outcomes. *Science*, *356*(6345). https://doi.org/10.1126/science.aal2324

Robertson, G. P., Hamilton, S. K., Paustian, K., & Smith, P. (2022). Land-based climate solutions for the United States. *Global Change Biology*, *28*, 4912–4919. https://doi.org/10.1111/gcb.16267

Saby, N. P. A., Arrouays, D., Antoni, V., Lemercier, B., Follain, S., Walter, C., & Schvartz, C. (2008). Changes in soil organic carbon in a mountainous French region, 1990–2004. *Soil Use and Management*, *24*(3), 254–262. https://doi.org/10.1111/j.1475-2743.2008.00159.x

Schmer, M. R., Vogel, K. P., Mitchell, R. B., & Perrin, R. K. (2008). Net energy of cellulosic ethanol from switchgrass. *Proceedings of the National Academy of Sciences of the United States of America*, *105*(2), 464–469. https://doi.org/10.1073/pnas.0704767105

Schmer, M. R., Vogel, K. P., Varvel, G. E., Follett, R. F., Mitchell, R. B., & Jin, V. L. (2014). Energy potential and greenhouse gas emissions from bioenergy cropping systems on marginally productive cropland. *PLoS One*, *9*(3), e89501. https://doi.org/10.1371/journal.pone.0089501

Slessarev, E. W., Nuccio, E. E., McFarlane, K. J., Ramon, C. E., Saha, M., Firestone, M. K., & Pett-Ridge, J. (2020). Quantifying the effects of switchgrass (Panicum virgatum) on deep organic C stocks using natural abundance ^{14}C in three marginal soils. *GCB Bioenergy*, *12*, 834–847. https://doi.org/10.1111/gcbb.12729

Sohn, J., Kalbar, P., Goldstein, B., & Birkved, M. (2020). Defining temporally dynamic life cycle assessment: A review. *Integrated Environmental Assessment and Management*, *16*(3), 314–323. https://doi.org/10.1002/ieam.4235

Sokhansanj, S., Mani, S., Tagore, S., & Turhollow, A. F. (2010). Techno-economic analysis of using corn Stover to supply heat and power to a corn ethanol plant—Part 1: Cost of feedstock supply logistics. *Biomass & Bioenergy*, *34*(1), 75–81. https://doi.org/10.1016/j.biombioe.2009.10.001

Sollins, P., Homann, P., & Caldwell, B. A. (1996). Stabilization and destabilization of soil organic matter: Mechanisms and controls. *Geoderma*, *74*(1), 65–105. https://doi.org/10.1016/S0016-7061(96)00036-5

Tao, L., Schell, D., Davis, R., Tan, E., Elander, R., & Bratis, A. (2014). *NREL 2012 achievement of ethanol cost targets: Biochemical ethanol fermentation via dilute-acid pretreatment and enzymatic hydrolysis of corn Stover*. NREL/TP-5100-61563 United States 10.2172/1129271, National Renewable Energy Laboratory. https://www.osti.gov/servlets/purl/1129271

Tao, L., Tan, E. C. D., McCormick, R., Zhang, M., Aden, A., He, X., & Zigler, B. T. (2014). Techno-economic analysis and life-cycle assessment of cellulosic isobutanol and comparison with cellulosic ethanol and n-butanol. *Biofuels Bioproducts & Biorefining-Biofpr*, *8*(1), 30–48. https://doi.org/10.1002/bbb.1431

Tilman, D., Hill, J., & Lehman, C. (2006). Carbon-negative biofuels from low-input high-diversity grassland biomass. *Science*, *314*(5805), 1598–1600. https://doi.org/10.1126/science.1133306

Tiruta-Barna, L., Pigné, Y., Gutiérrez, N. T., & Benetto, E. (2016). Framework and computational tool for the consideration of time dependency in life cycle inventory. Proof of concept. *Journal of Cleaner Production*, *116*, 198–206.

U.S. Department of Energy. (2016). *2016 Billion-ton report: Advancing domestic resources for a thriving bioeconomy, Vol. 1: Economic availability of feedstocks (ORNL/TM-2016/160)*. https://www.energy.gov/eere/bioenergy/downloads/2016-billion-ton-report-advancing-domestic-resources-thriving-bioeconomy

U.S. Department of Transportation. (2015). *2012 commodity flow survey*. https://www.bts.gov/archive/publications/commodity_flow_survey/2012/united_states/index

U.S. Energy Information Administration. (2018). *Form EIA-923 detailed data with previous form data (EIA-906/920)*. https://www.eia.gov/electricity/data/eia923/

U.S. Energy Information Administration. (2019). *Annual energy outlook 2019*.

U.S. Environmental Protection Agency. (2010). *Regulation of fuels and fuel additives: Changes to renewable fuel standard program; final rule*. https://www.gpo.gov/fdsys/pkg/FR-2010-03-26/pdf/2010-3851.pdf

U.S. Environmental Protection Agency. (2018). *Emissions & generation resource integrated database eGRID2016*.

Valdez, Z. P., Hockaday, W. C., Masiello, C. A., Gallagher, M. E., & Robertson, G. P. (2017). Soil carbon and nitrogen responses to nitrogen fertilizer and harvesting rates in switchgrass cropping systems. *Bioenergy Research*, *10*, 456–464. https://doi.org/10.1007/s12155-016-9810-7

Wang, M., Han, J., Dunn, J. B., Cai, H., & Elgowainy, A. (2012). Well-to-wheels energy use and greenhouse gas emissions of ethanol from corn, sugarcane and cellulosic biomass for US use. *Environmental Research Letters*, *7*(4). https://doi.org/10.1088/1748-9326/7/4/045905

Werling, B. P., Dickson, T. L., Isaacs, R., Gaines, H., Gratton, C., Gross, K. L., Liere, H., Malmstrom, C. M., Meehan, T. D., Ruan, L., Robertson, B. A., Robertson, G. P., Schmidt, T. M., Schrotenboer, A. C., Teal, T. K., Wilson, J. K., & Landis, D. A. (2014). Perennial grasslands enhance biodiversity and multiple ecosystem services in bioenergy landscapes. *Proceedings of the National Academy of Sciences of the United States of America*, *111*(4), 1652–1657. https://doi.org/10.1073/pnas.1309492111

Won, W., Motagamwala, A. H., Dumesic, J. A., & Maravelias, C. T. (2017). A co-solvent hydrolysis strategy for the production of biofuels: Process synthesis and technoeconomic analysis. *Reaction Chemistry & Engineering*, *2*(3), 397–405. https://doi.org/10.1039/c6re00227g

Wright, L., & Turhollow, A. (2010). Switchgrass selection as a "model" bioenergy crop: A history of the process. *Biomass & Bioenergy*, *34*(6), 851–868. https://doi.org/10.1016/j.biombioe.2010.01.030

Yang, J., & Chen, B. (2014). Global warming impact assessment of a crop residue gasification project a dynamic LCA perspective. *Applied Energy*, *122*, 269–279. https://doi.org/10.1016/j.apenergy.2014.02.034

Yuan, C., Wang, E., Zhai, Q., & Yang, F. (2015). Temporal discounting in life cycle assessment. A critical review and theoretical framework. *Environmental Impact Assessment Review*, *51*, 23–31.

Zhao, G., Bryan, B. A., King, D., Luo, Z., Wang, E., Song, X., & Yu, Q. (2013). Impact of agricultural management practices on soil organic carbon: Simulation of Australian wheat systems. *Global Change Biology*, *19*(5), 1585–1597. https://doi.org/10.1111/gcb.12145

SUPPORTING INFORMATION

Additional supporting information can be found online in the Supporting Information section at the end of this article.

How to cite this article: Kim, S., Dale, B. E., Martinez-Feria, R., Basso, B., Thelen, K., Maravelias, C. T., Landis, D., Lark, T. J., & Robertson, G. P. (2023). Global warming intensity of biofuel derived from switchgrass grown on marginal land in Michigan. *GCB Bioenergy*, *00*, 1–13. https://doi.org/10.1111/gcbb.13024

Supplementary Material: Global Warming intensity of biofuel derived from switchgrass grown on marginal land in Michigan

Seungdo Kim*[1,2], Bruce E. Dale[1,2], Rafael Martinez-Feria[1,3], Bruno Basso[1,3,4], Kurt Thelen[1,5], Christos T. Maravelias[6,7,8], Douglas Landis[1,9], Tyler J. Lark[8,10], G. Philip Robertson[1,4,11]

[1]DOE Great Lakes Bioenergy Research Center, Michigan State University, East Lansing, MI 48824, USA

[2] Department of Chemical Engineering and Materials Science, Michigan State University, East Lansing, MI, 48824, USA

[3] Department of Earth and Environmental Science, Michigan State University, East Lansing, MI, 48824, USA

[4] W. K. Kellogg Biological Station, Michigan State University, Hickory Corners, MI, 49060, USA

[5] Department of Plant, Soil and Microbial Sciences, Michigan State University, East Lansing, MI 48824, USA

[6] Department of Chemical and Biological Engineering, Princeton University, Princeton, NJ 08540, USA

[7] Andlinger Center for Energy and Environment, Princeton University, Princeton, NJ 08540, USA

[8] DOE Great Lakes Bioenergy Research Center, University of Wisconsin-Madison, Madison, WI 53726, USA

[9] Department of Entomology, Michigan State University, East Lansing, MI 48824, USA

[10] Nelson Institute Center for Sustainability and the Global Environment (SAGE), University of Wisconsin-Madison, WI 53726, USA

[11] Department of Plant, Soil and Microbial Sciences, Michigan State University, East Lansing, MI, 48824, USA

Corresponding author:

Seungdo Kim

Phone: 1-517-355-4621

Email: kimseun@egr.msu.edu

Table S1. Assumptions

Switchgrass planting cycle	11 years (establishing year and continuous culture for 10 years)
Agronomic inputs	N: 50 kgN/ha for 50N, 0 kgN/ha for 0N P: 2 kgP_2O_5/dry Mg harvested[1] K: 7 kgK_2O/dry Mg harvested[1] Herbicides[a]: 2.78 kg a.i./ha before planting 1.72 kg a.i./ha in the 1st year 2.13 kg a.i./ha in the 2nd year 1.08 kg a.i./ha in the 3rd year
Harvest	Switchgrass is harvested in October. no harvest if a land parcel is not able to produce one biomass bale (540 dry kg)
Potential marginal lands for biofuel production	No forest and wet marginal lands prior to the land use conversion No marginal lands in islands Harvest frequency>=0.9
Dry mass loss[2]	Field Treatment loss: 2% Field Drying loss: 5% Harvest/Collection loss: 3% Farm Handling loss: 2% Loss in storage: 8.4% Loss in transport: 2%
Time horizon	30 years
Collection radius	80.5 km (50 miles)
Transport of biofuel from biorefinery to bulk terminal[2]	Barge (3.2%): 837 km Railroad (78.9%): 1287 km Truck (7.9%): 128.7 km
Transport of biofuel from bulk terminal to refueling station[2]	Truck (100%): 48 km

a DOE Great Lakes Bioenergy Research Center (GLBRC) marginal land experimental sites in Michigan (https://data.sustainability.glbrc.org/datatables)

Table S2. Process information

	Unit	CHEM[3]	ACID[4]	GREET[2]
Biofuel yield	liter/dry Mg	286	296	355
Input materials				
Sulfuric acid	g/liter	343	91	91
Sodium hydroxide (caustic soda)	g/liter		30.43	31.10
Ammonia	g/liter		15.09	10.98
Corn steep liquor	g/liter		41.42	34.76
Diammonium phosphate	g/liter		4.26	3.66
Sorbitol	g/liter		1.34	
Glucose	g/liter		95.51	
Host nutrients	g/liter		2.68	
Sulfur dioxide	g/liter		0.65	
Polymer	g/liter		0.32	
Boiler water chemicals	g/liter		0.01	
FGD lime	g/liter		19.72	20.12
Cooling tower chemicals	g/liter		0.08	
Makeup water	g/liter		6612	
Antifoam agent	g/liter		0.53	
Toluene	g/liter	3.84		
Lime (Calcium hydroxide)	g/liter	259		
Cellulase	g/liter			28.19
Yeast	g/liter	0.47		7.02
RuSn4/C catalyst	g/liter	0.00		
WWT Nutrients	g/liter	1.32		
CaO	g/liter			20.12
Urea	g/liter			5.49
Diesel	liter/liter			0.0001
Excess electricity	kwh/liter	0.76	0.70	0.64
Emissions to air				
CH_4	g/liter	0.13	0.12	0.67
N_2O	g/liter			0.42

Table S3. Results in the dynamic approach (The SOC sequestration rate and GWI are weighted averages based on marginal land parcel area and biofuel volume, respectively.)

Year	Ethanol (GL year^{-1})	SOC sequestration rate (Mg C ha^{-1} year^{-1})	GWI (g CO_2 MJ^{-1})		GHG mitigation (Tg CO_2 year^{-1})	
			P_EIA	P_COAL	P_EIA	P_COAL
1	0.14	-0.87 (±0.77)	441.68 (±307.36)	441.68 (±307.36)	-1.02	-1.02
2	0.34	-0.4 (±0.61)	89.1 (±73.61)	89.1 (±73.61)	0.03	0.03
3	0.54	-0.2 (±0.46)	41.19 (±34.5)	41.19 (±34.5)	0.59	0.59
4	0.74	0.09 (±0.28)	13.06 (±15.64)	13.1 (±15.64)	1.26	1.26
5	0.70	0.26 (±0.27)	1.91 (±16.03)	1.91 (±16.03)	1.35	1.35
6	0.72	0.33 (±0.27)	-3.04 (±15.65)	-3.04 (±15.65)	1.48	1.48
7	0.60	0.38 (±0.24)	-9.54 (±17)	-9.54 (±17)	1.31	1.31
8	0.66	0.39 (±0.24)	-8.87 (±15.43)	-8.09 (±15.43)	1.43	1.42
9	0.69	0.37 (±0.22)	-6.1 (±14.14)	-4.65 (±14.14)	1.44	1.42
10	0.59	0.41 (±0.25)	-12.46 (±18.74)	-10.41 (±18.74)	1.33	1.3
11	0.73	1.38 (±0.17)	-74.3 (±11.37)	-71.66 (±11.37)	2.59	2.55
12	0.14	1.45 (±0.28)	-315.9 (±104.11)	-314.35 (±104.22)	1.21	1.21
13	0.26	0.3 (±0.21)	-22.33 (±42.73)	-18.35 (±42.78)	0.65	0.63
14	0.52	0.16 (±0.37)	4.06 (±26.3)	8.86 (±26.3)	0.99	0.94
15	0.64	0.23 (±0.27)	2.26 (±19.63)	7.62 (±19.63)	1.23	1.16
16	0.71	0.36 (±0.25)	-3.71 (±18.68)	2.08 (±18.68)	1.45	1.37
17	0.62	0.39 (±0.25)	-7.06 (±19.54)	-0.58 (±19.54)	1.33	1.24
18	0.69	0.41 (±0.26)	-6.99 (±18.08)	0.05 (±18.08)	1.46	1.36
19	0.59	0.43 (±0.25)	-10.79 (±19.23)	-3.5 (±19.23)	1.31	1.22
20	0.72	0.37 (±0.22)	-4 (±15.23)	3.21 (±15.23)	1.49	1.38
21	0.75	0.39 (±0.21)	-4.27 (±13.01)	2.82 (±13.01)	1.56	1.45
22	0.71	1.52 (±0.15)	-84.35 (±11.13)	-77.34 (±11.13)	2.67	2.56
23	0.08	1.64 (±0.29)	-415.58 (±134.44)	-414.96 (±135.42)	0.9	0.9
24	0.26	0.21 (±0.28)	-59.19 (±106.36)	-53.65 (±107.37)	0.86	0.82
25	0.53	0.08 (±0.37)	14.77 (±29.91)	21.5 (±29.92)	0.89	0.81
26	0.69	0.24 (±0.27)	5.05 (±20.32)	11.75 (±20.32)	1.28	1.19
27	0.67	0.29 (±0.26)	3.58 (±19.85)	10.19 (±19.85)	1.28	1.19
28	0.63	0.31 (±0.27)	4.86 (±28.99)	11.42 (±28.99)	1.18	1.09
29	0.76	0.33 (±0.23)	0.98 (±15.07)	7.51 (±15.07)	1.5	1.39
30	0.59	0.43 (±0.2)	-8.66 (±16.58)	-2.25 (±16.58)	1.29	1.2

Table S4. Comparison of GWI (Unit: g CO_2 MJ^{-1})

GHG sources	CHEM	ACID	GREET	Chen et al.[5]
Agronomic inputs/fuel/N_2O	22.95	22.17	18.50	16.67
SOC	-34.45	-33.26	-27.46	-15.5
Transport/storage	3.46	3.34	2.79	
Biorefinery	17.00	18.28	16.46	10.06
surplus electricity	-20.25	-18.68	-17.05	-13.54
Biofuel distribution/combustion	1.94	1.94	1.94	4
GWI	-9.35	-6.22	-4.81	1.69

Figure S1. State of Michigan (colored by yellow) [created with the Maptitude mapping software, www.caliper.com]

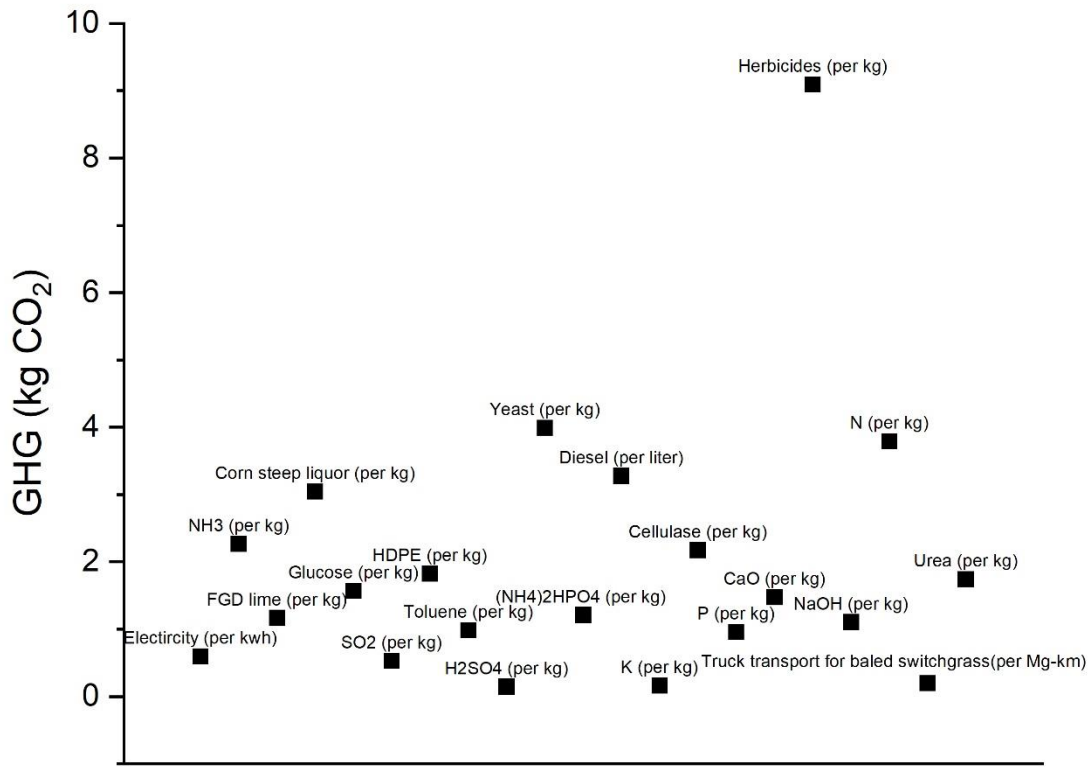

Figure S2. Cumulative GHG emissions of materials and fuels

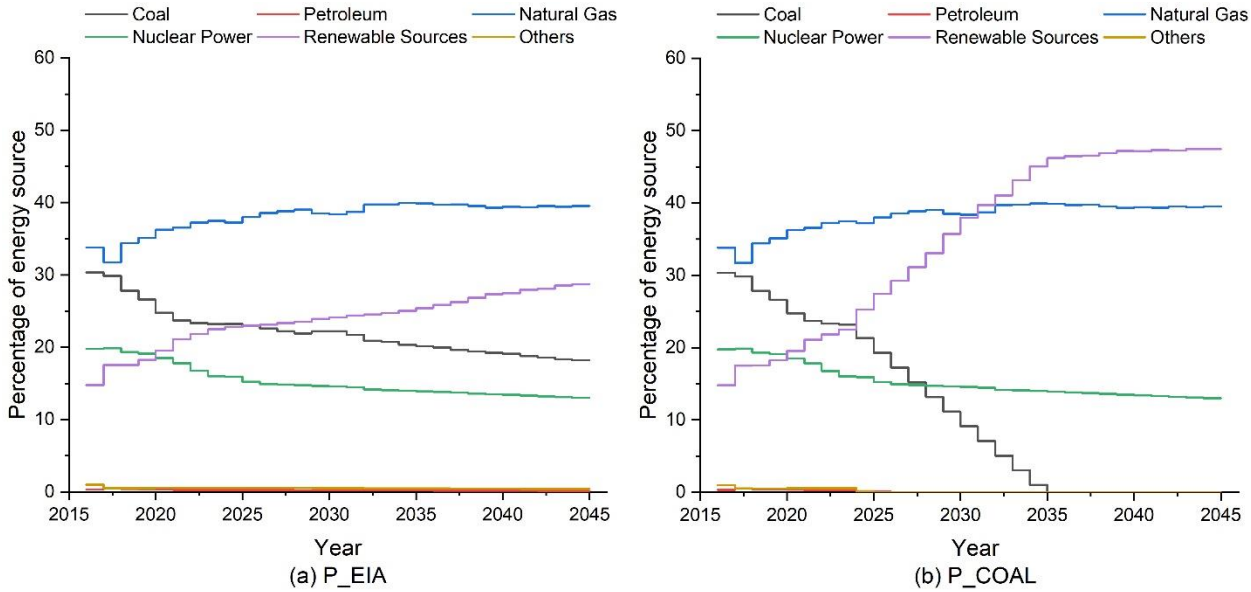

Figure S3. Projected electricity fuel mixes.

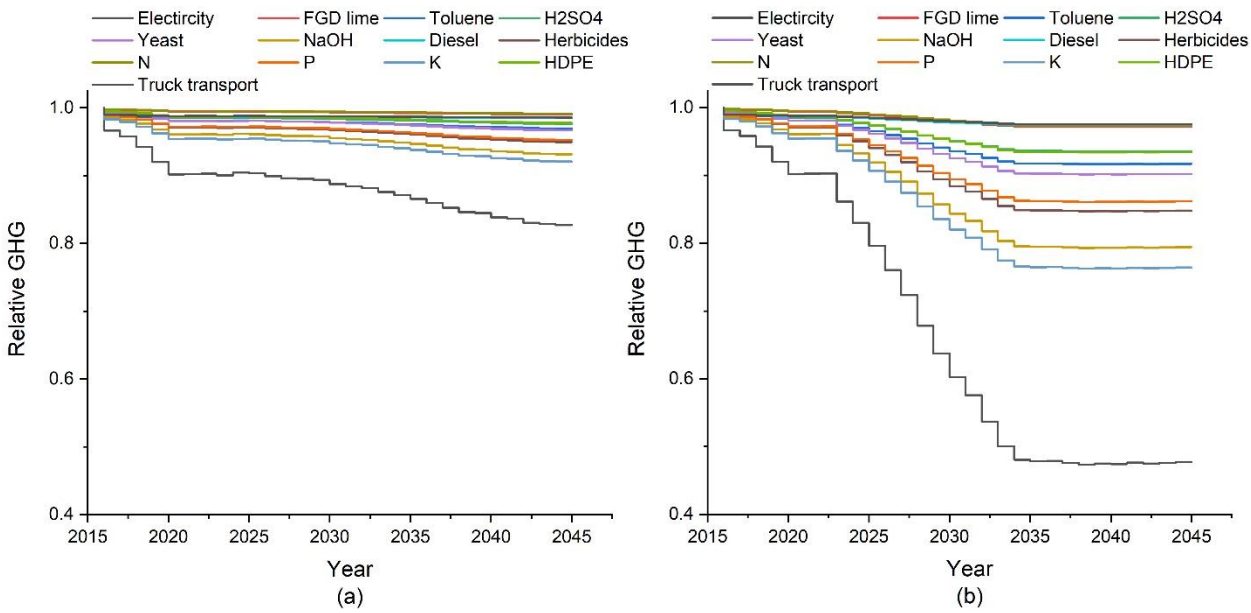

Figure S4. Relative time-dependent GHG emissions, equal to the ratio of GHG in the ith year to GHG in year 2016. (a) P_EIA and (b) P_COAL

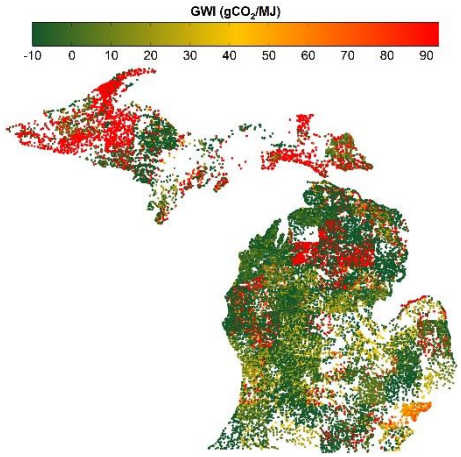

CHEM for 0N

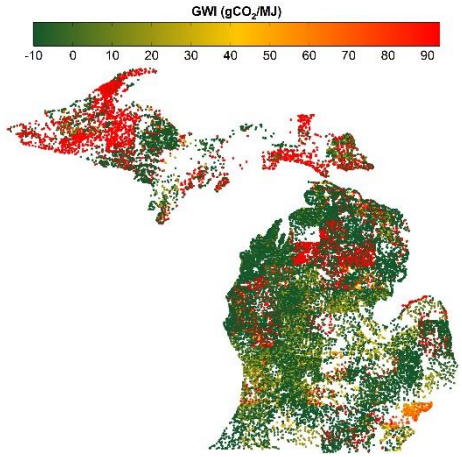

CHEM for 50N

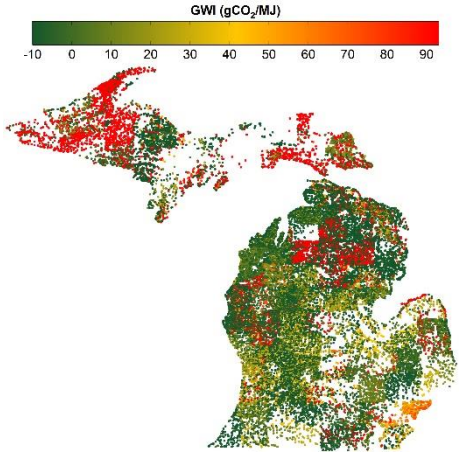

ACID for 0N

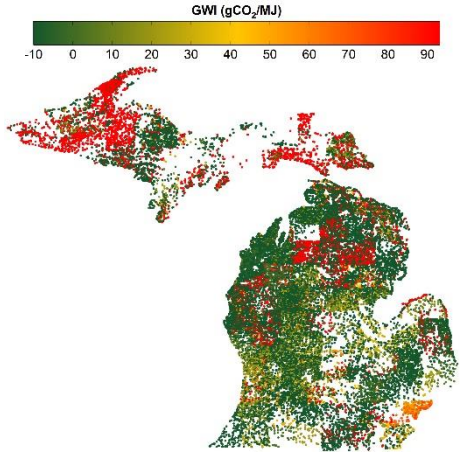

ACID for 50N

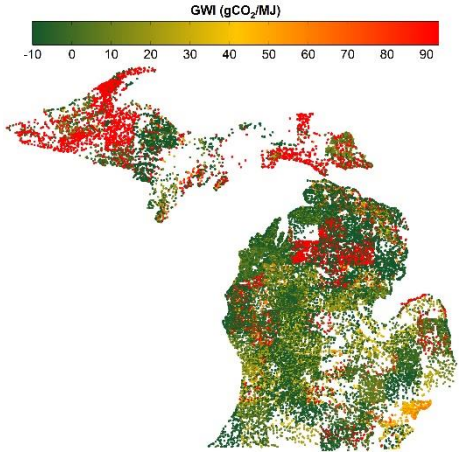

GREET for 0N

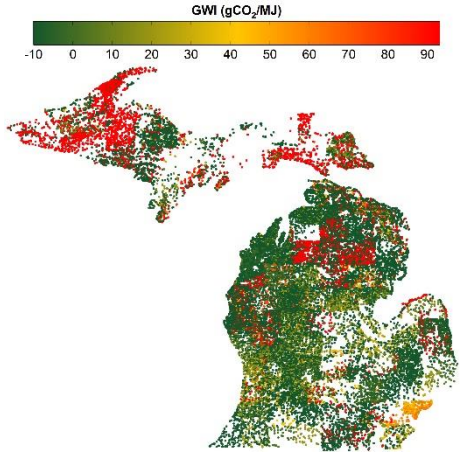

GREET for 50N

Figure S5. Spatial static GWI.

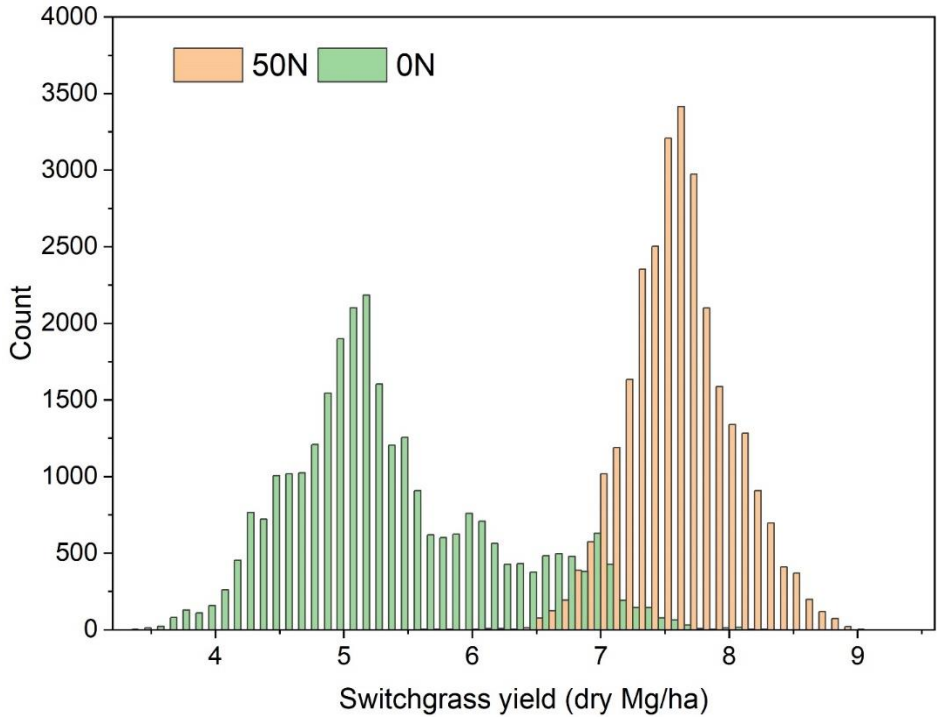

Figure S6. Switchgrass yield

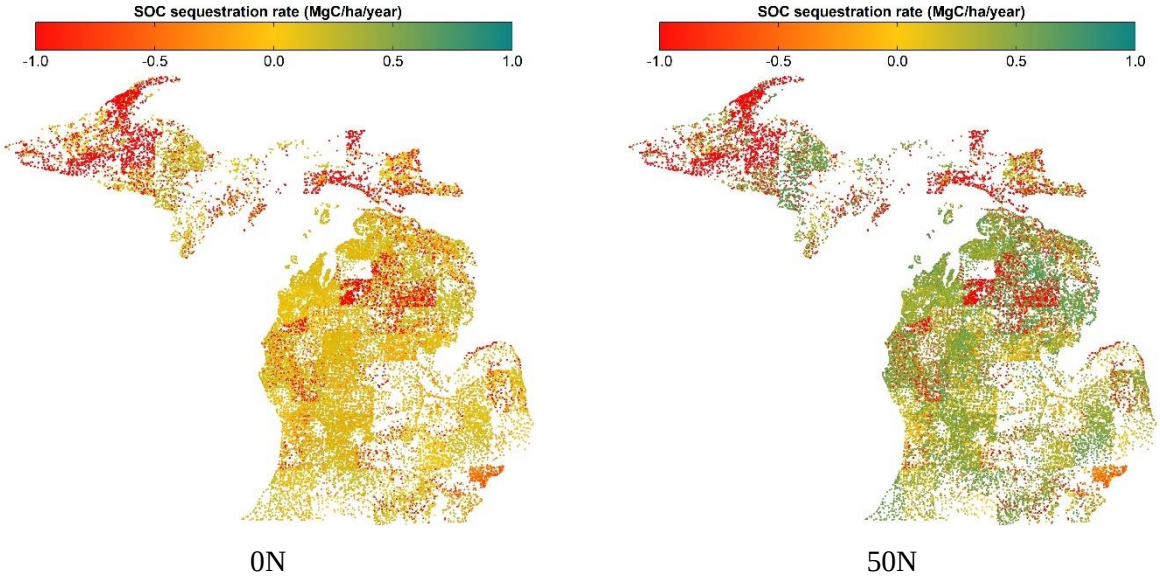

Figure S7. Average SOC sequestration rate for individual parcels over a 30-year period.

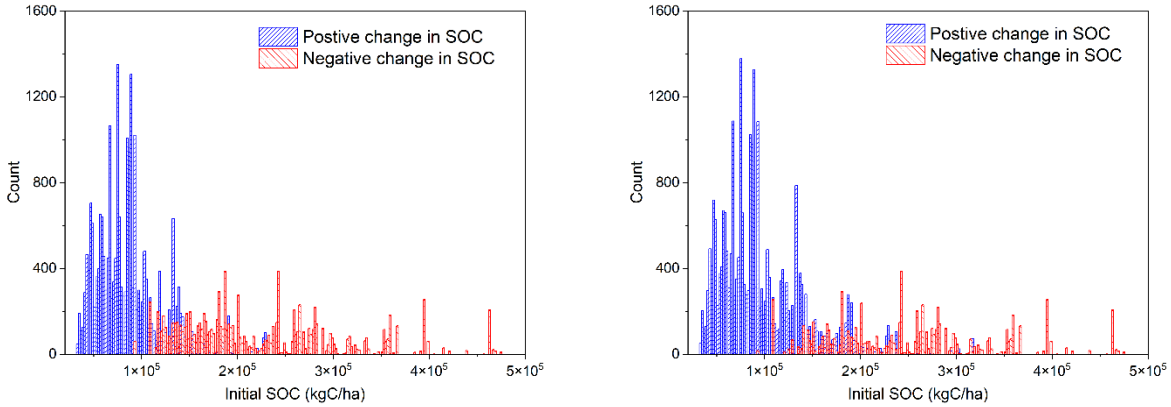

0N 50N

Figure S8. Effects of the Initial SOC stock on SOC change for individual parcels

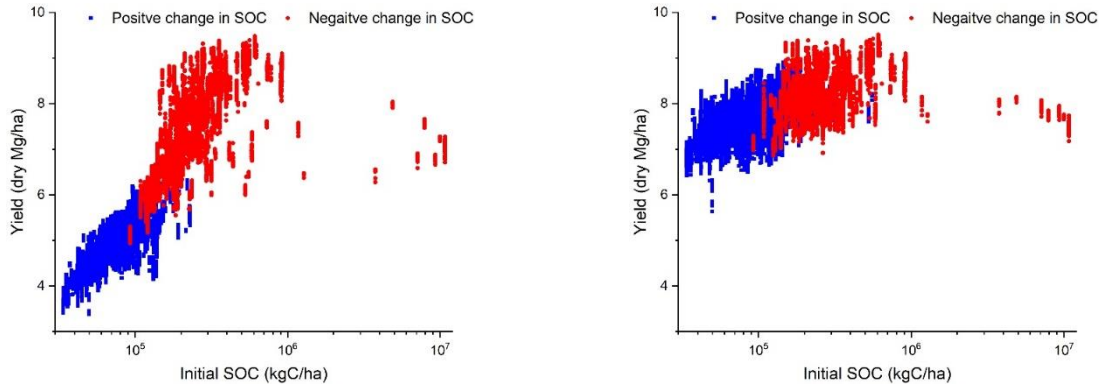

0N 50N

Figure S9. Effect of biomass yield on SOC change

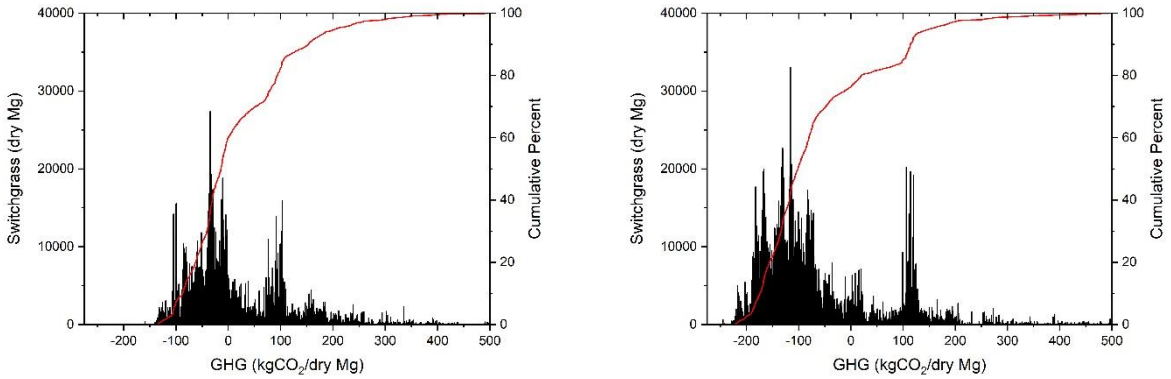

0N 50N

Figure S10. Distribution of static GHG emissions of switchgrass (The black vertical lines represent the amount of switchgrass, and the red lines represent the cumulative percentage.)

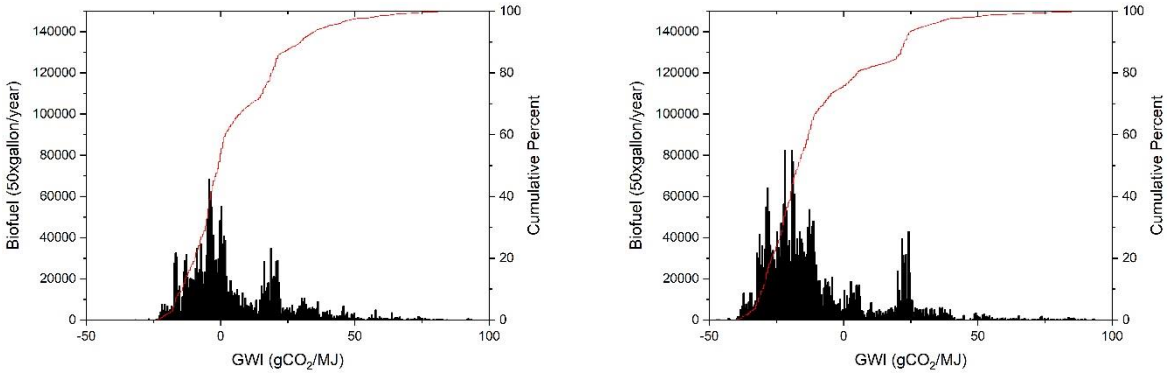

0N 50N

Figure S11. Distribution of static GWI of biofuel produced through the CHEM model (50 gallons = 189 L, The black vertical lines represent the volume of biofuel, and the red lines represent the cumulative percentage.)

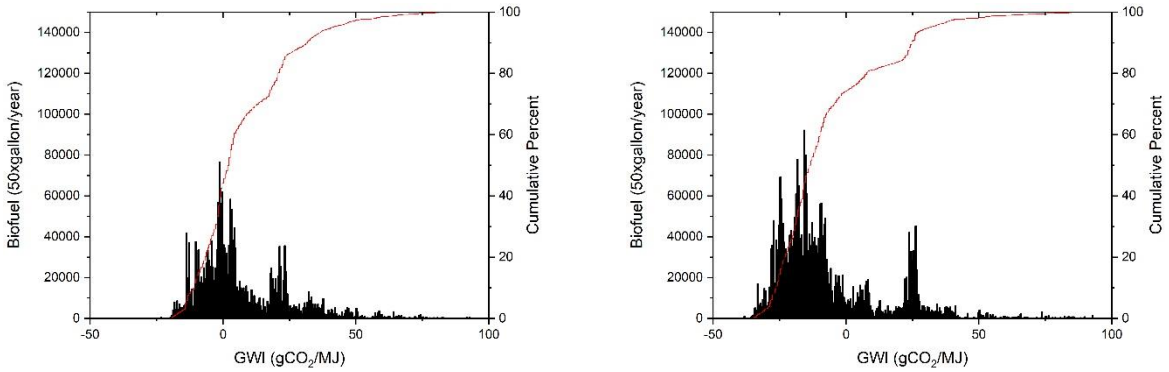

0N 50N

Figure S12. Distribution of static GWI of biofuel produced through the ACID model (50 gallons = 189 L, The black vertical lines represent the volume of biofuel, and the red lines represent the cumulative percentage.)

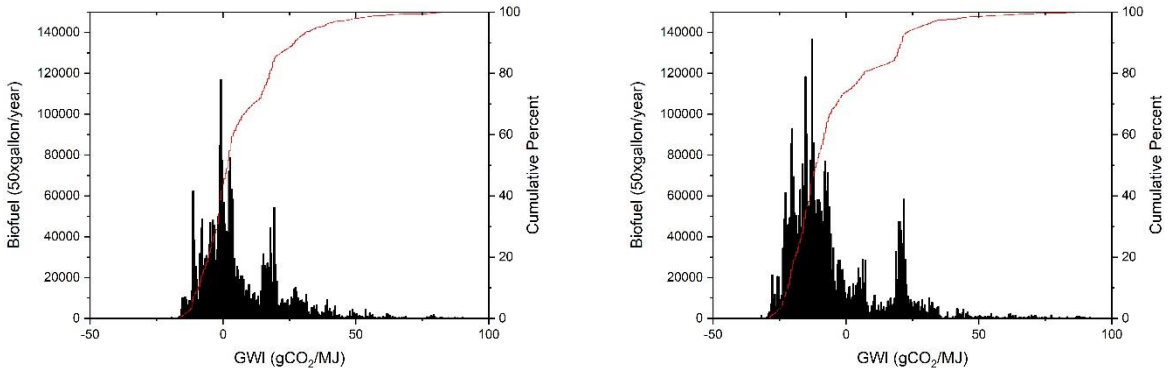

0N 50N

Figure S13. Distribution of static GWI of biofuel produced through the GREET model (50 gallons = 189 L, The black vertical lines represent the volume of biofuel, and the red lines represent the cumulative percentage.)

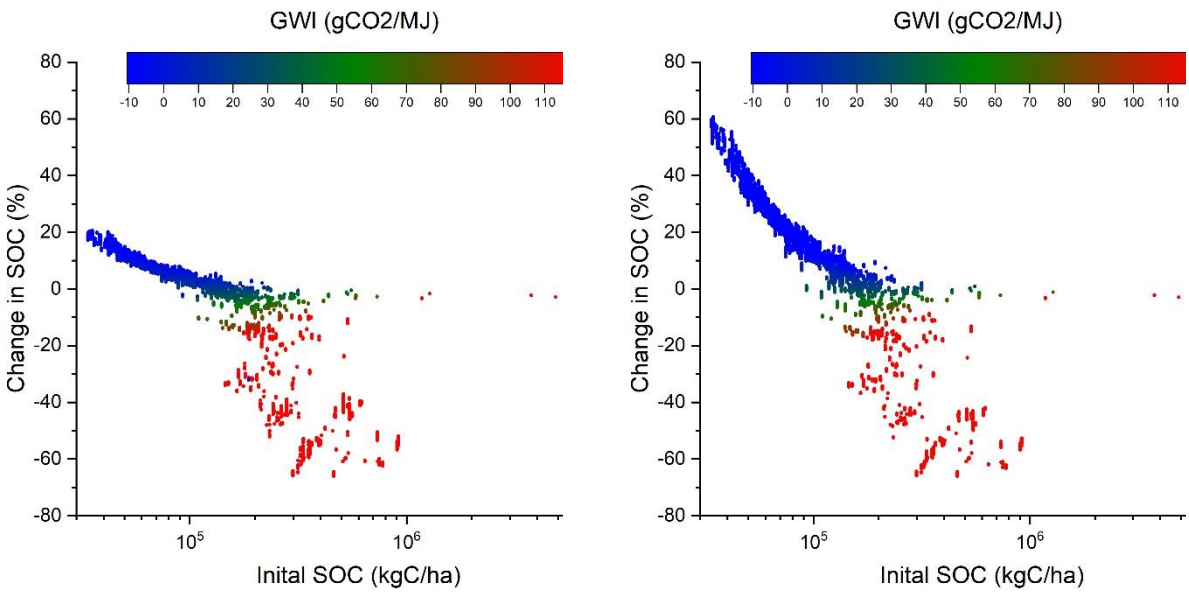

0N 50N

Figure S14. Initial SOC stock, change in SOC and GWI in the CHEM model

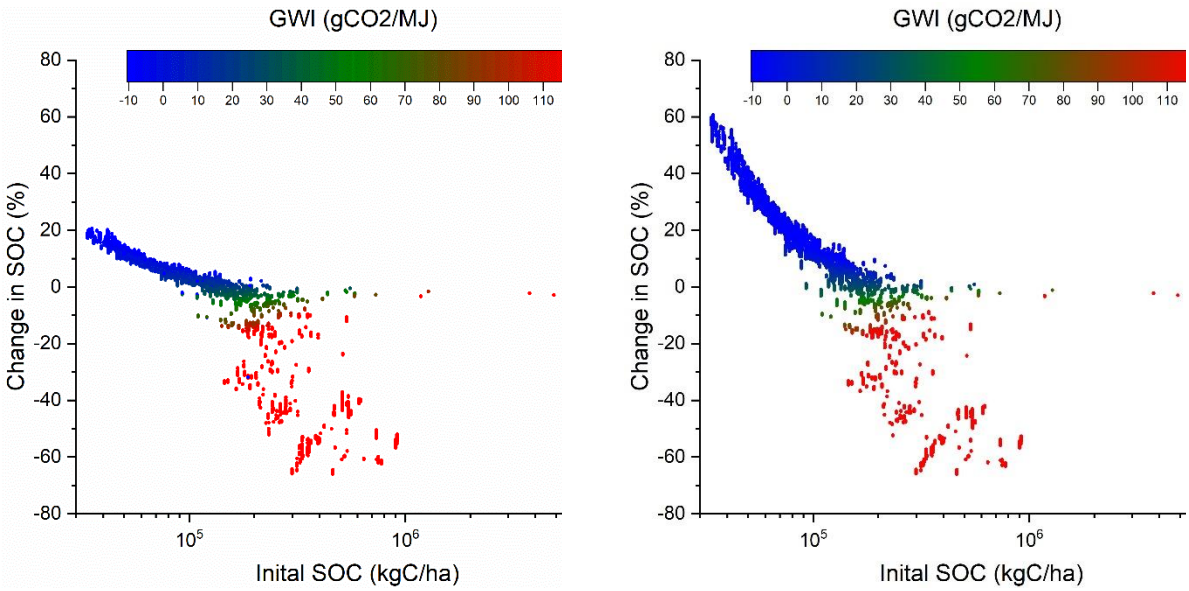

0N 50N

Figure S15. Initial SOC stock, change in SOC and GWI in the ACID model

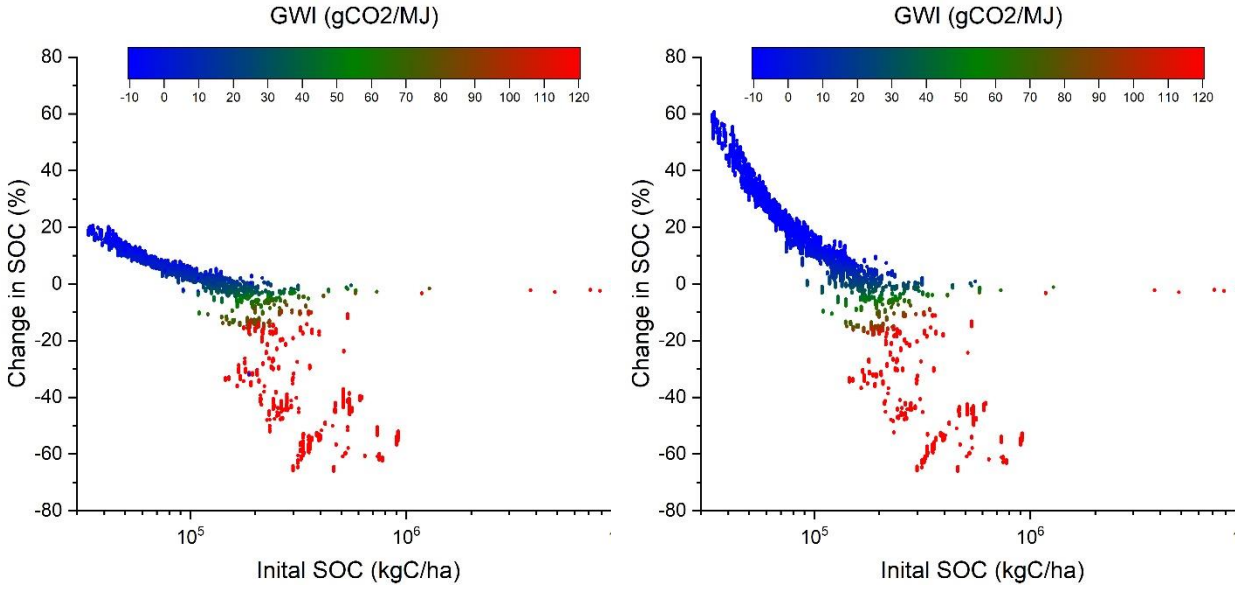

0N 50N

Figure S16. Initial SOC stock, change in SOC and GWI in the GREET model

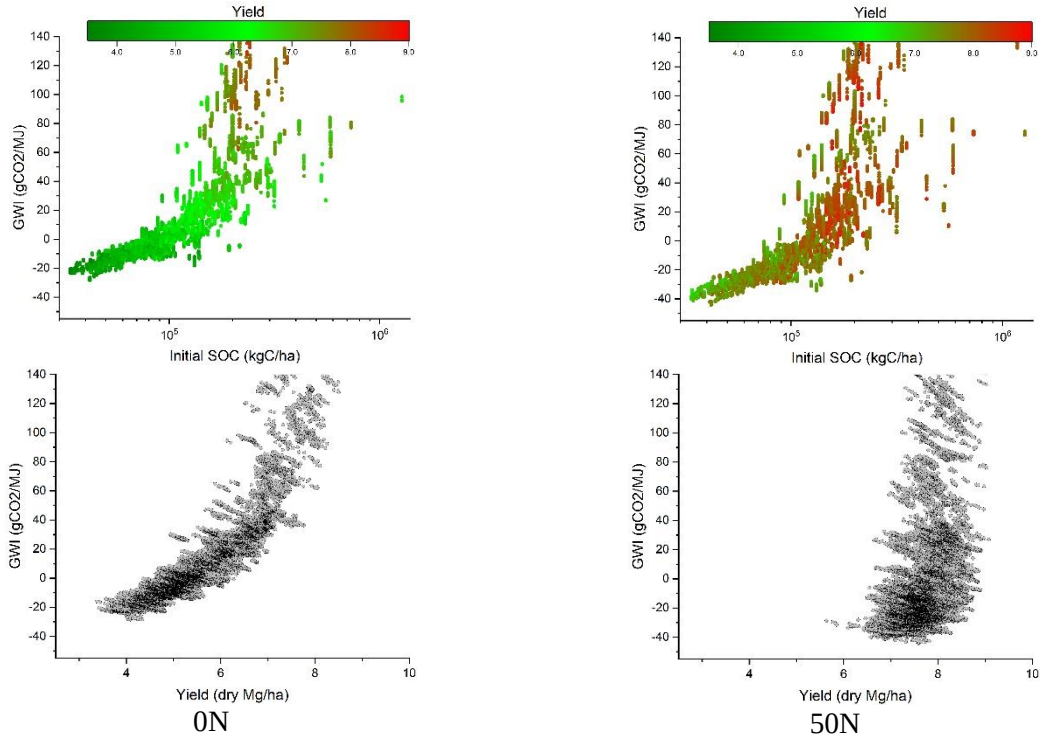

Figure S17. Initial SOC stock, biomass yield and GWI in the CHEM model

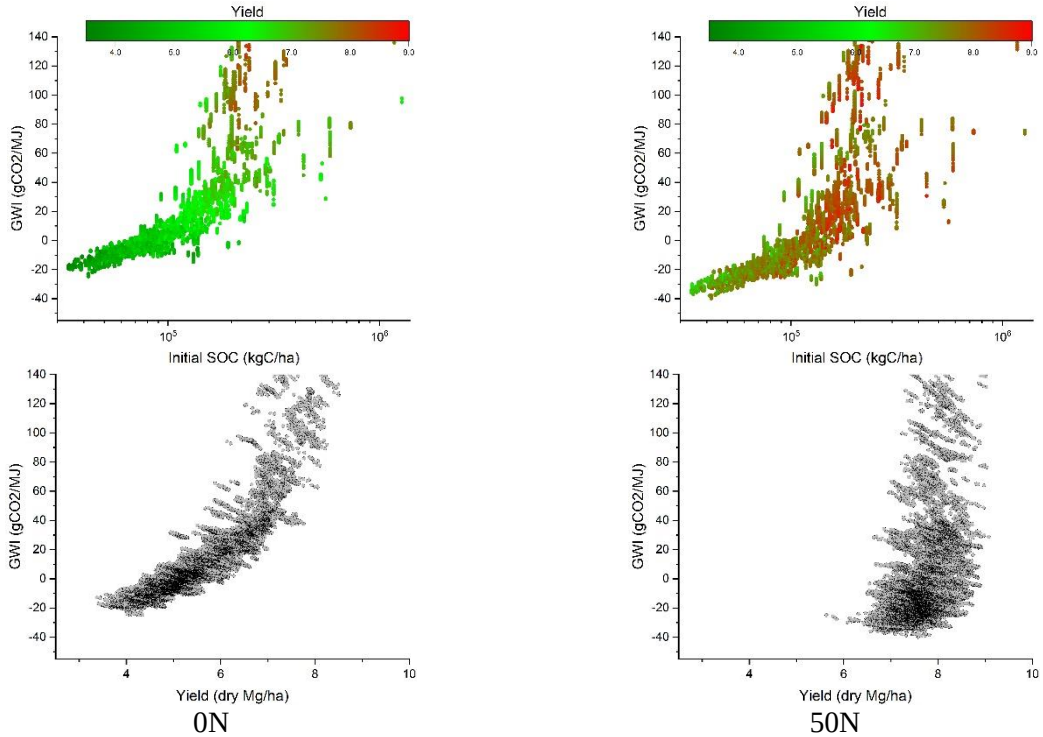

Figure S18. Initial SOC stock, biomass yield and GWI in the ACID model

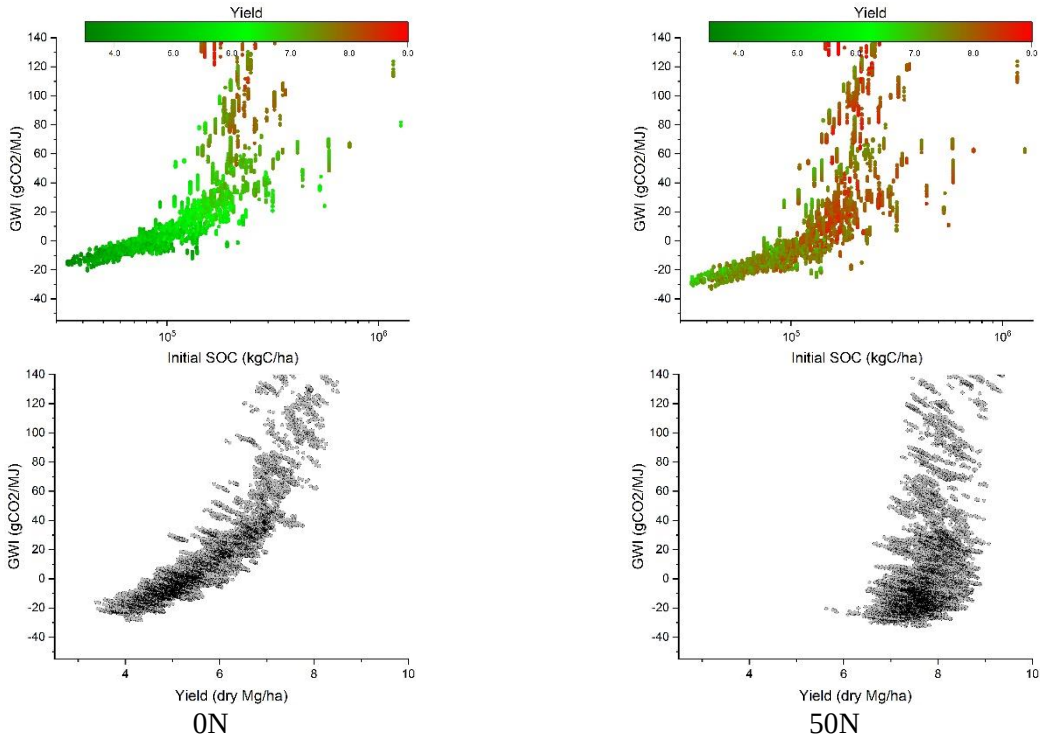

Figure S19. Initial SOC stock, biomass yield and GWI in the GREET model

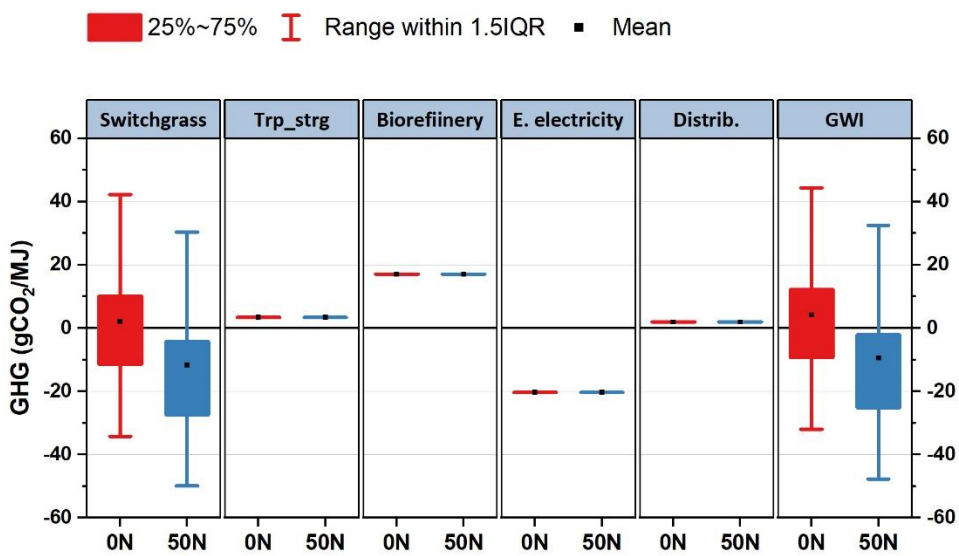

Figure S20. Breakdown of the static GWI of biofuel produced through the CHEM model. "Switchgrass" is GHG emissions of switchgrass. "Trp" is GHG emissions associated with transport of baled switchgrass and storage facility. "Biorefinery" is GHG emissions from biorefinery, including materials and process emissions. "E. electricity" is GHG avoidance from the surplus electricity. "Distrib." is GHG emissions of distribution of biofuel and combustion. (IQR: interquartile range)

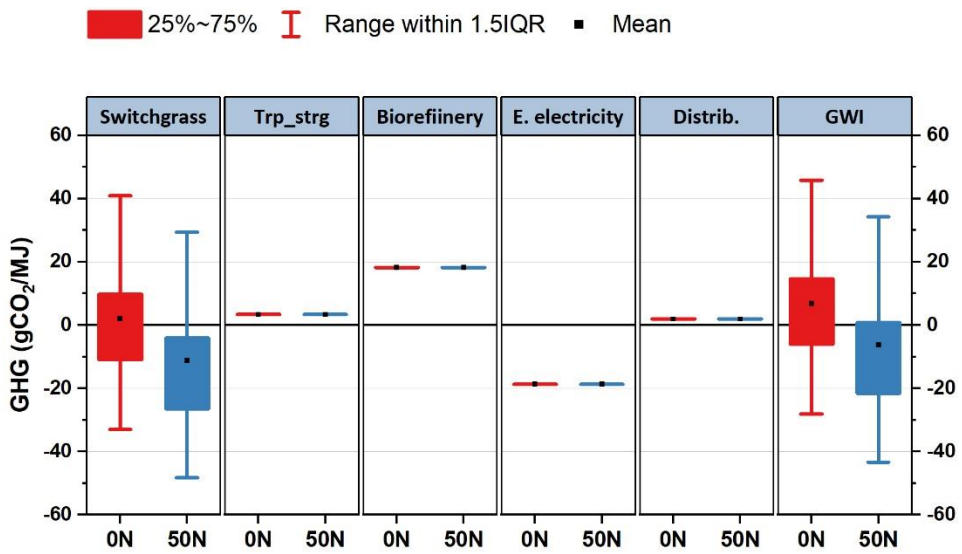

Figure S21. Breakdown of the static GWI of biofuel produced through the ACID model. "Switchgrass" is GHG emissions of switchgrass. "Trp_strg" is GHG emissions associated with transport of baled switchgrass and storage facility. "Biorefinery" is GHG emissions from biorefinery, including materials and process emissions. "E. electricity" is GHG avoidance from the surplus electricity. "Distrib." is GHG emissions of distribution of biofuel and combustion. (IQR: interquartile range)

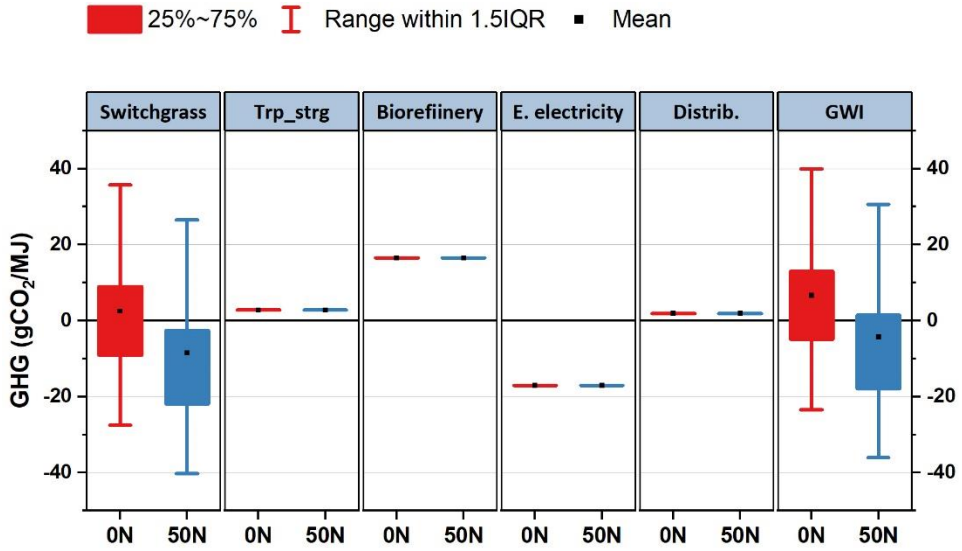

Figure S22. Breakdown of the static GWI of biofuel produced through the GREET model. "Switchgrass" is GHG emissions of switchgrass. "Trp_strg" is GHG emissions associated with transport of baled switchgrass and storage facility. "Biorefinery" is GHG emissions from biorefinery, including materials and process emissions. "E. electricity" is GHG avoidance from the surplus electricity. "Distrib." is GHG emissions of distribution of biofuel and combustion. (IQR: interquartile range)

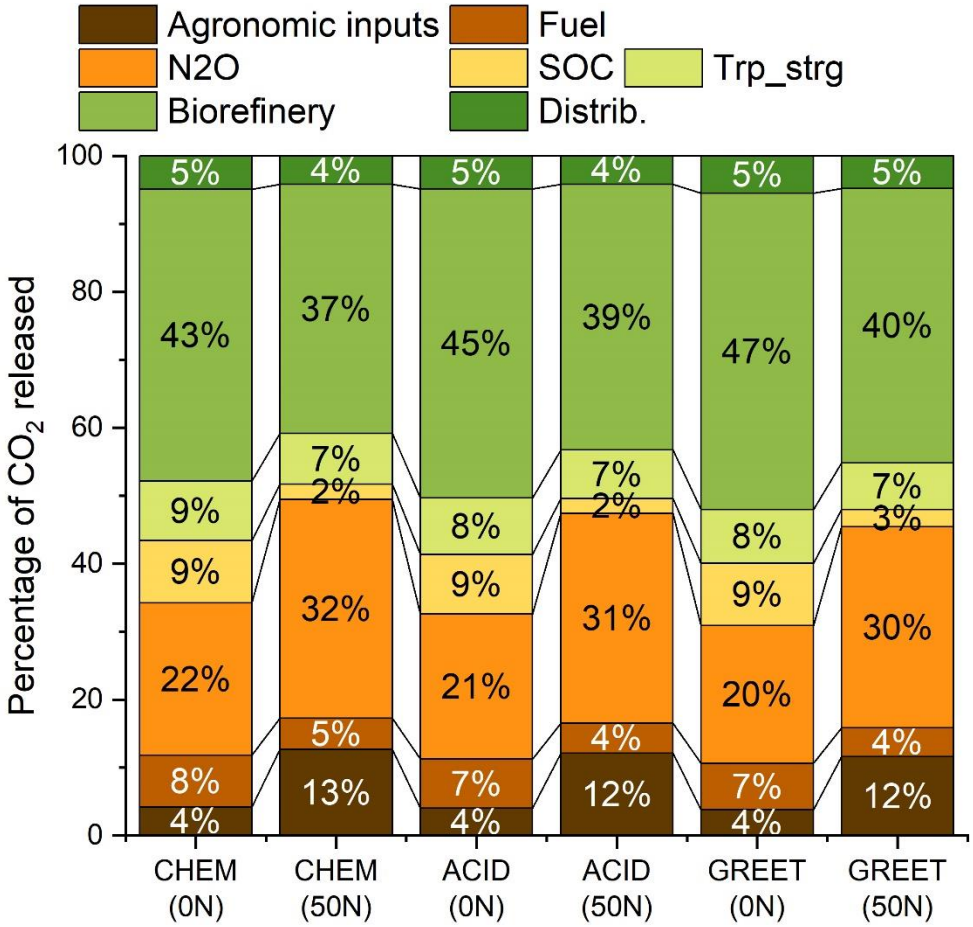

Figure S23. Ratios of GHG sources to GHG emissions released in the biofuel production. "Agronomic inputs" include GHG emissions of fertilizers (N, P, K), seed and herbicides. "Fuel" is GHG emissions associated with diesel used in field operations. "N2O" is N_2O emissions. "SOC" is GHG emissions of SOC loss. "Biorefinery" is GHG emissions from biorefinery, including materials and process emissions. "Trp_strg" is GHG emissions associated with transport of baled switchgrass and storage facility. "Distrib." is GHG emissions of distribution of biofuel and combustion.

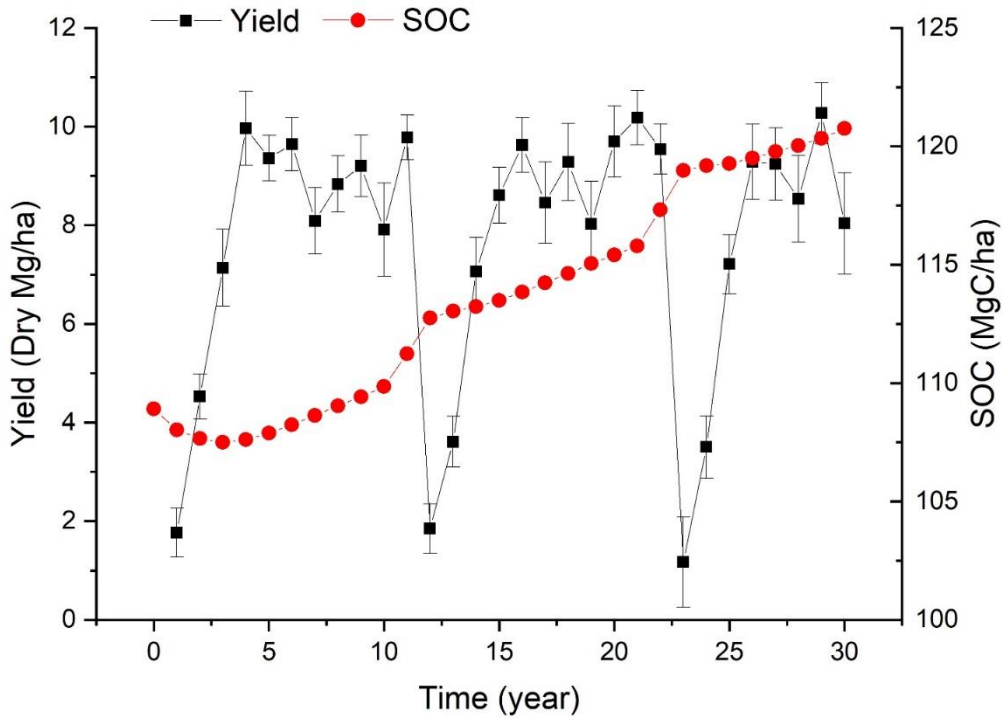

Figure S24. Switchgrass yields and SOC levels

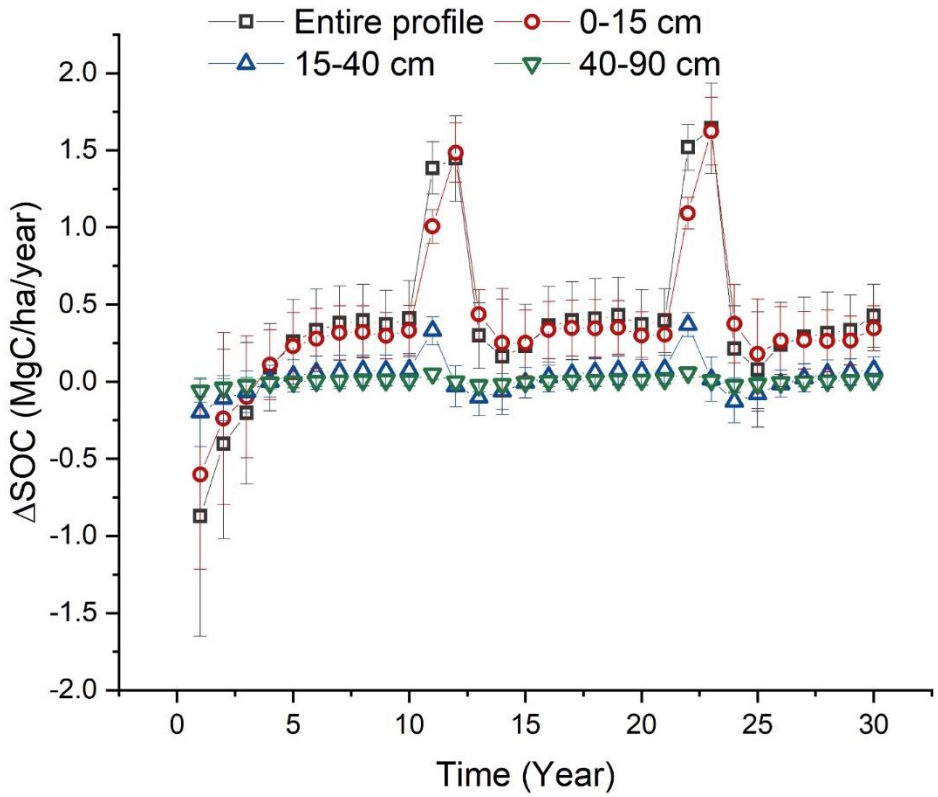

Figure S25. SOC sequestration rates with respect to soil depths

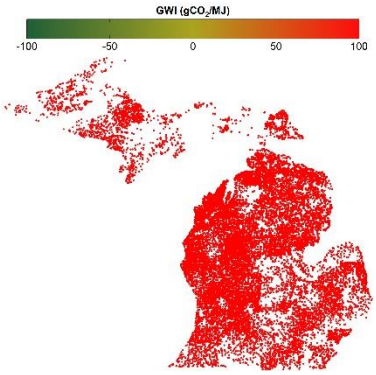

1st year in the first cycle

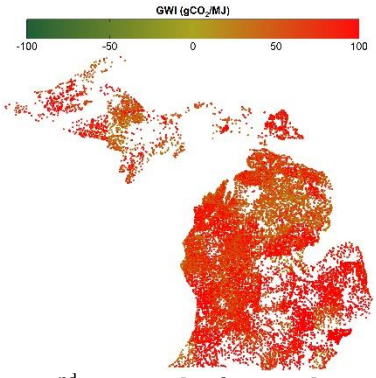

2nd year in the first cycle

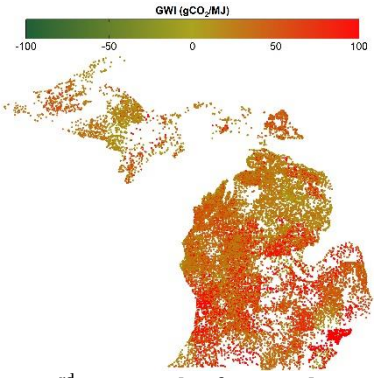

3rd year in the first cycle

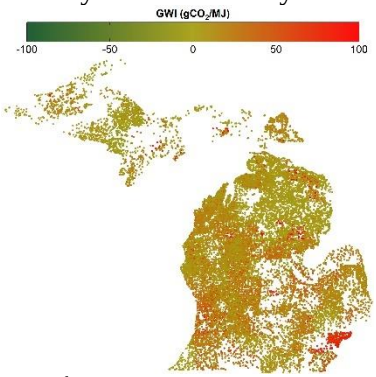

4th year in the first cycle

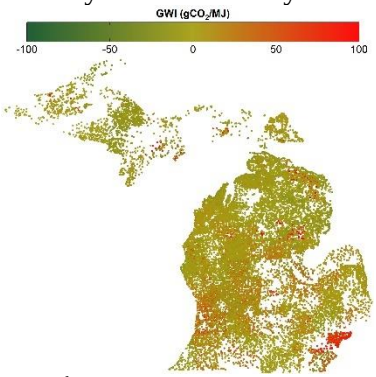

5th year in the first cycle

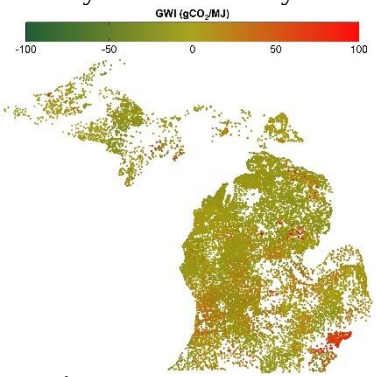

6th year in the first cycle

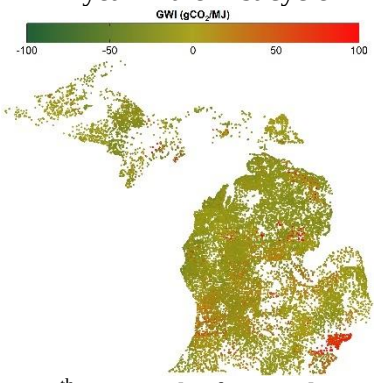

7th year in the first cycle

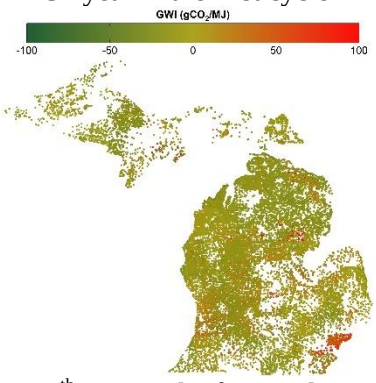

8th year in the first cycle

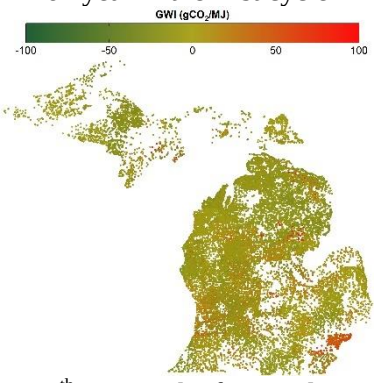

9th year in the first cycle

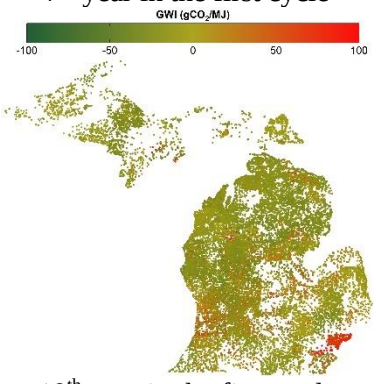

10th year in the first cycle

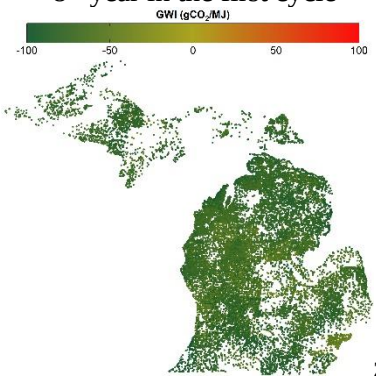

z

11th year in the first cycle

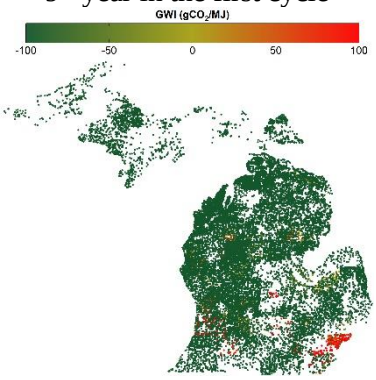

1st year in the second cycle

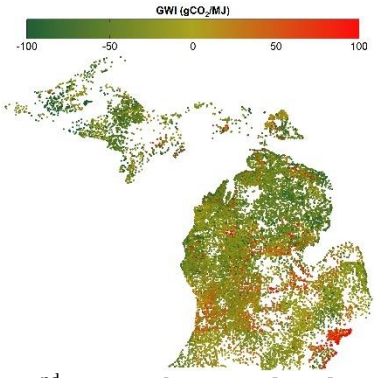

2nd year in the second cycle

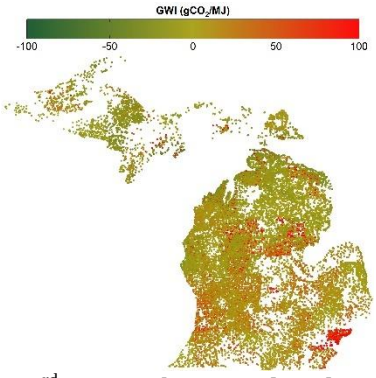

3rd year in the second cycle

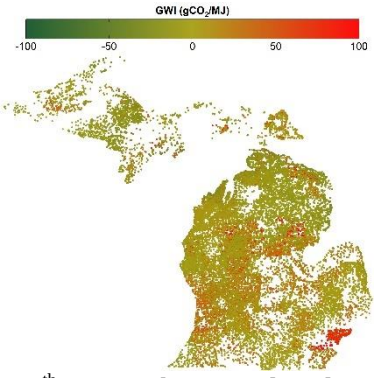

4th year in the second cycle

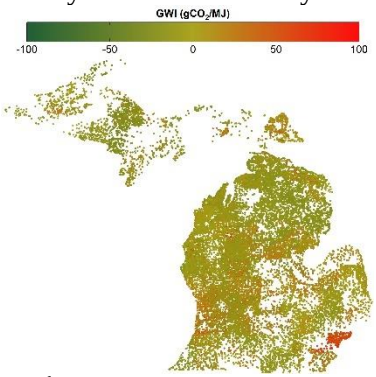

5th year in the second cycle

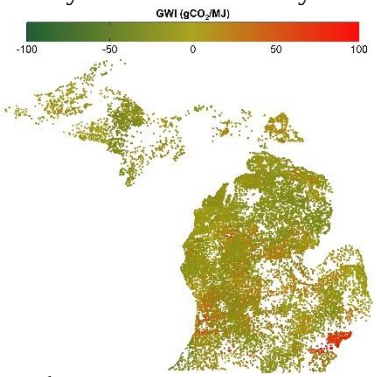

6th year in the second cycle

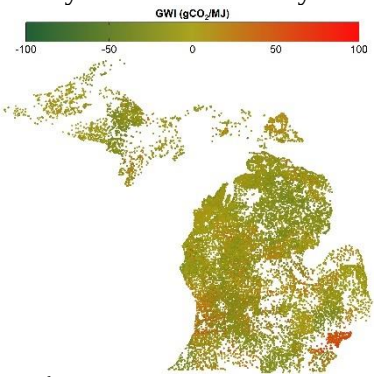

7th year in the second cycle

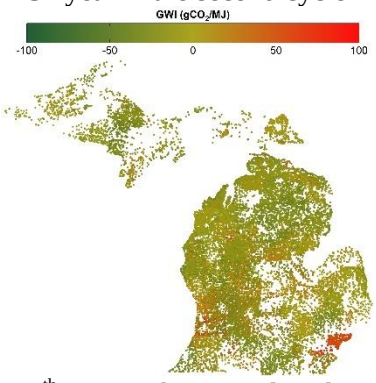

8th year in the second cycle

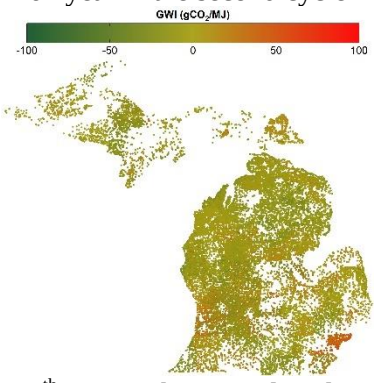

9th year in the second cycle

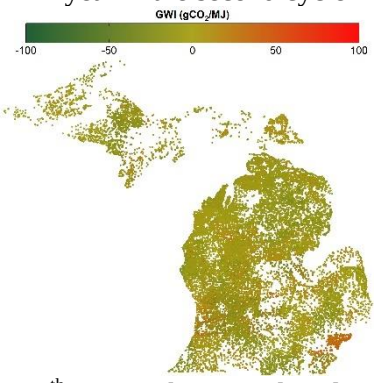

10th year in the second cycle

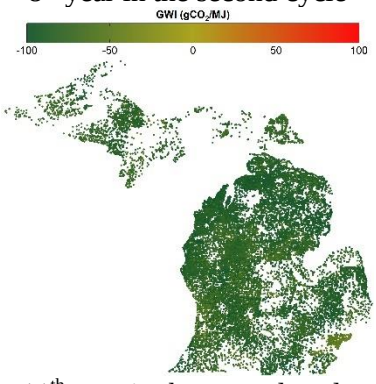

11th year in the second cycle

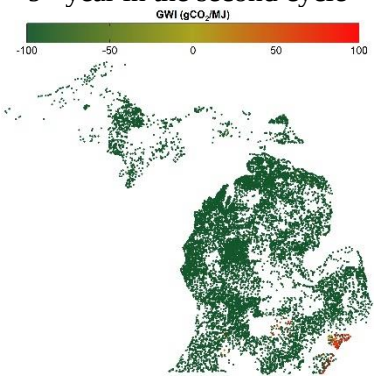

1st year in the third cycle

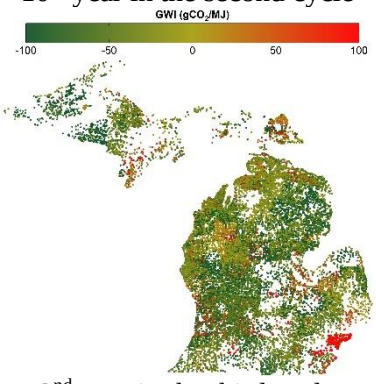

2nd year in the third cycle

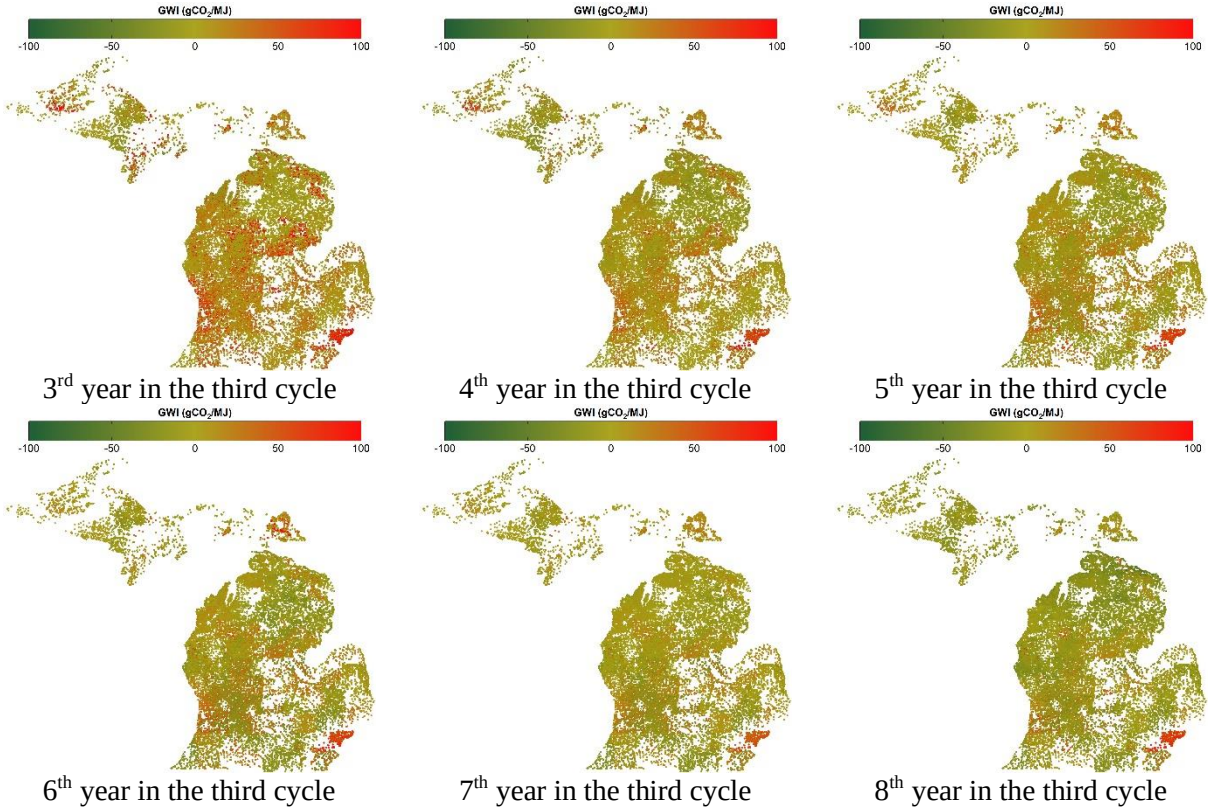

Figure S26. Dynamic GWIs based on the P_EIA projection (green color: <-100 g CO_2 MJ^{-1}, red color:>100 g CO_2 MJ^{-1})

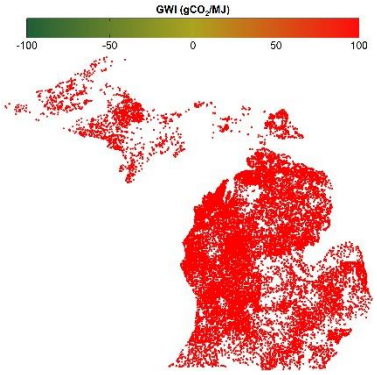

1st year in the first cycle

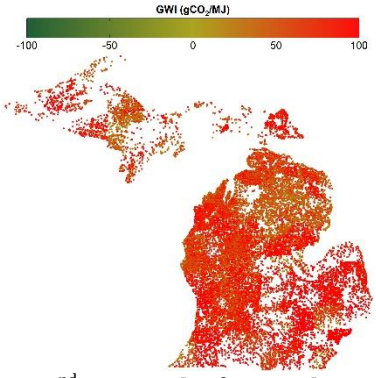

2nd year in the first cycle

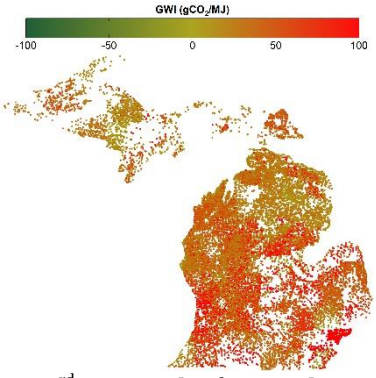

3rd year in the first cycle

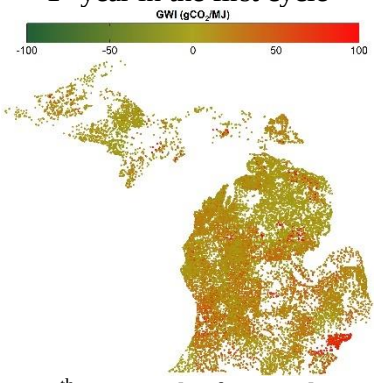

4th year in the first cycle

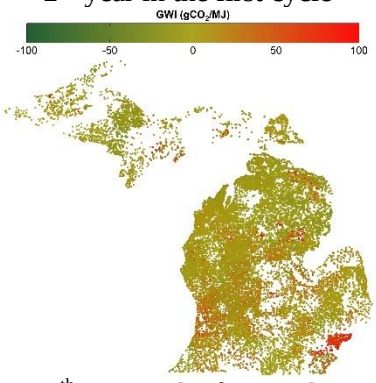

5th year in the first cycle

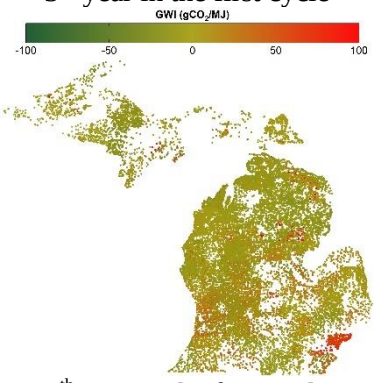

6th year in the first cycle

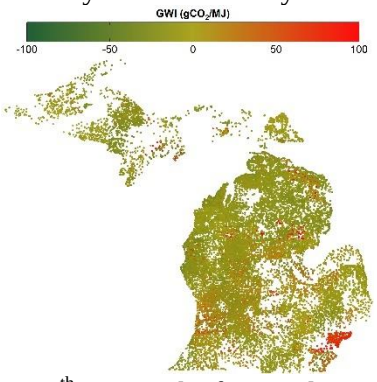

7th year in the first cycle

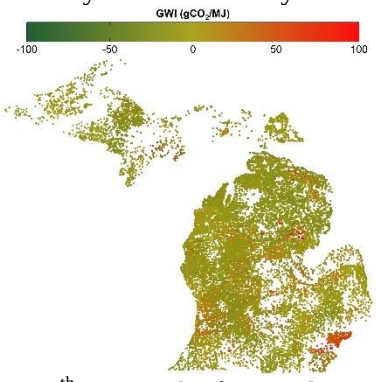

8th year in the first cycle

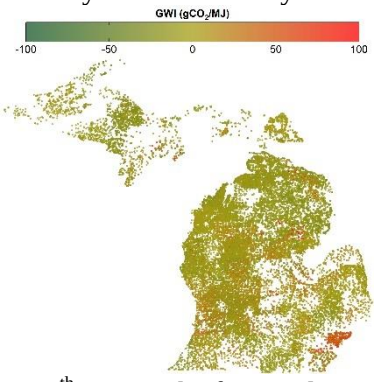

9th year in the first cycle

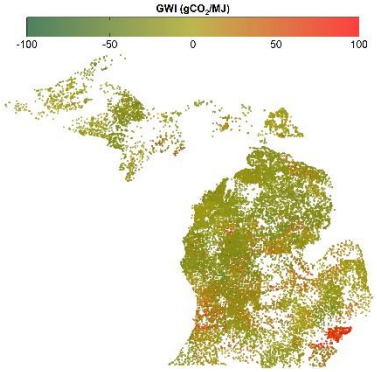

10th year in the first cycle

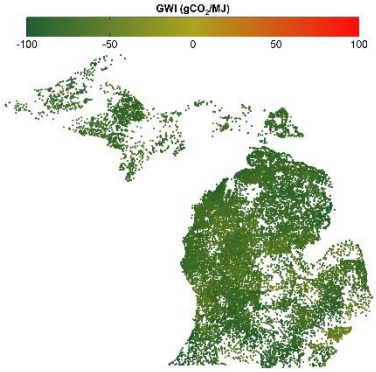

11th year in the first cycle

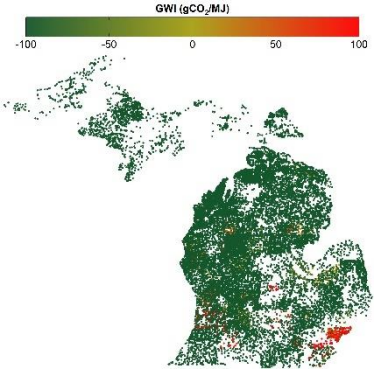

1st year in the second cycle

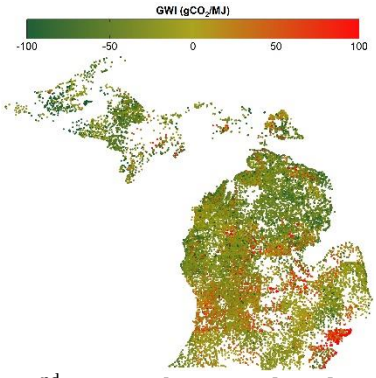

2nd year in the second cycle

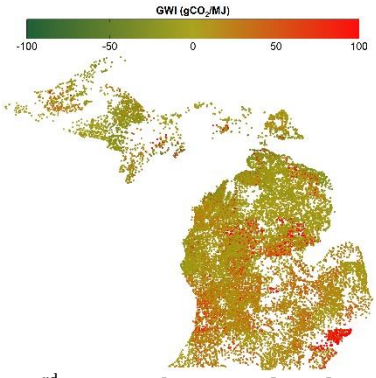

3rd year in the second cycle

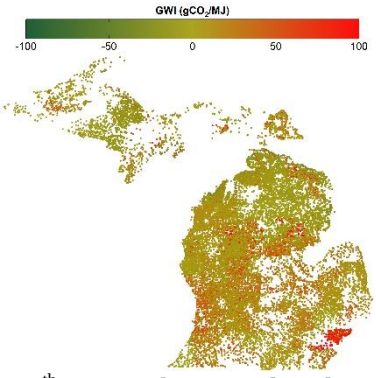

4th year in the second cycle

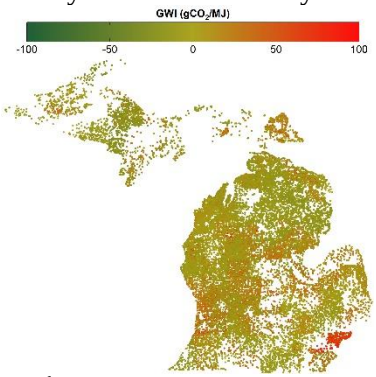

5th year in the second cycle

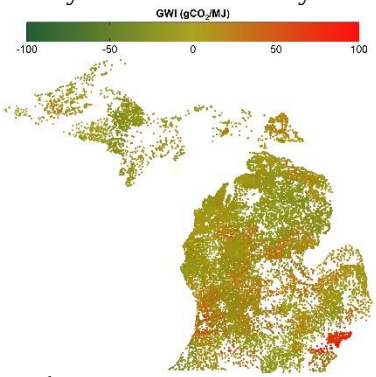

6th year in the second cycle

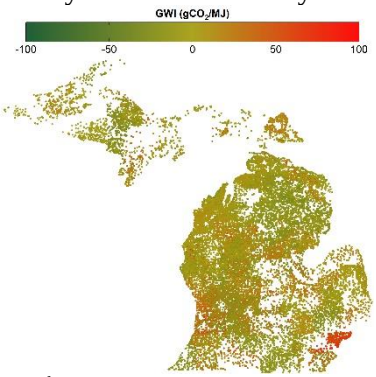

7th year in the second cycle

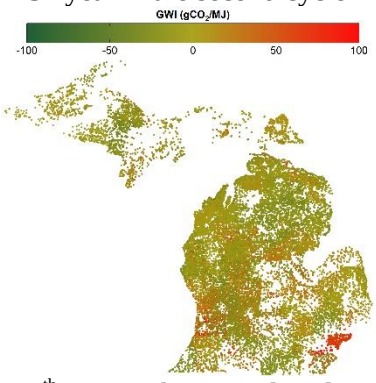

8th year in the second cycle

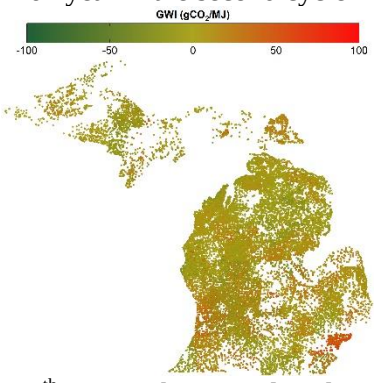

9th year in the second cycle

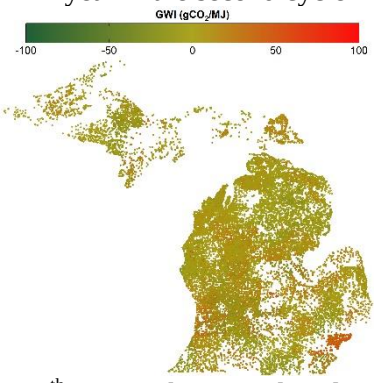

10th year in the second cycle

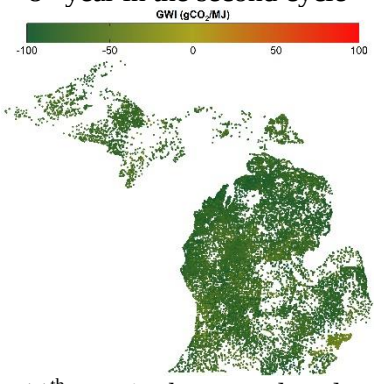

11th year in the second cycle

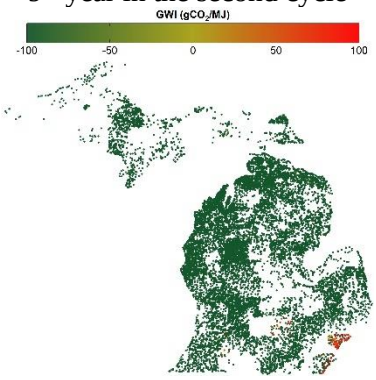

1st year in the third cycle

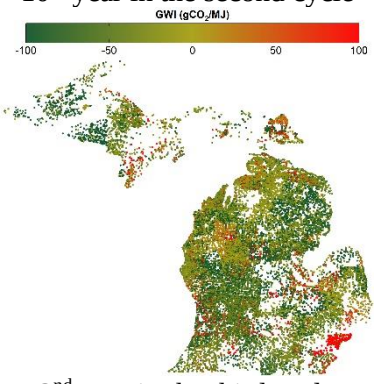

2nd year in the third cycle

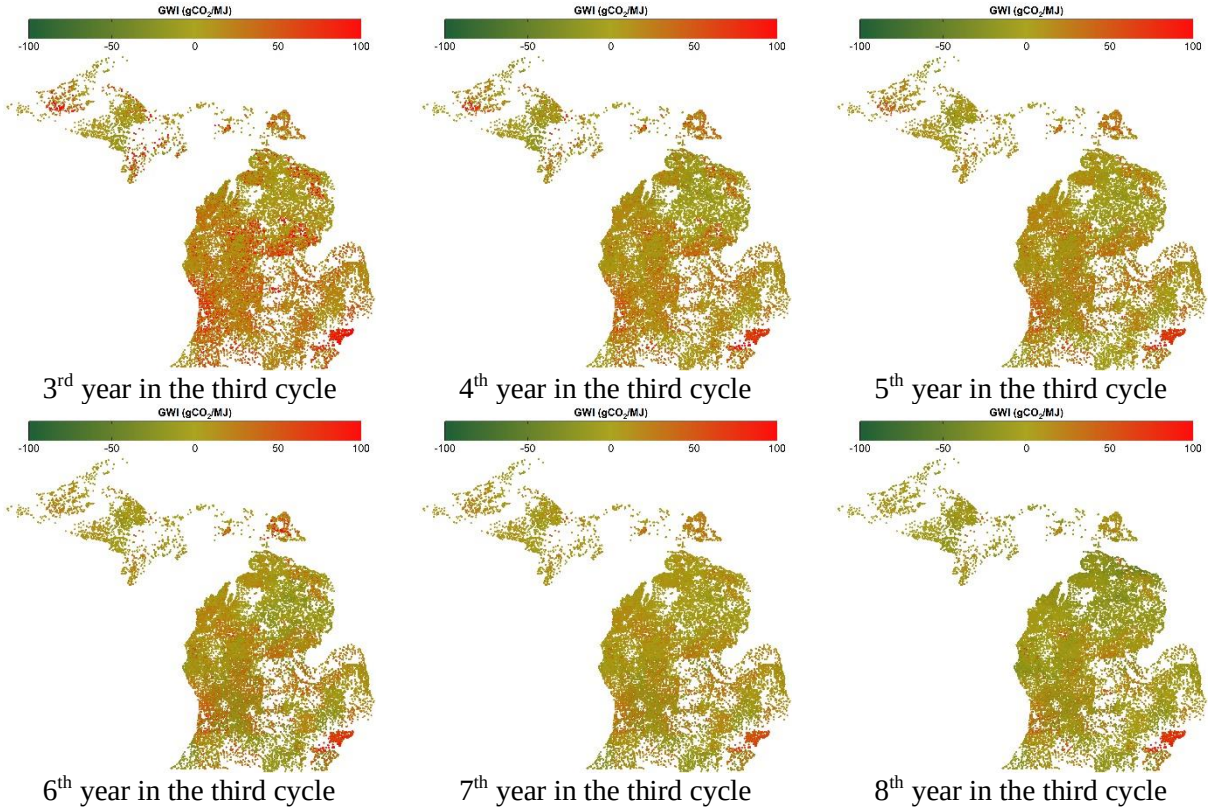

Figure S27. Dynamic GWIs based on the P_COAL projection (green color: <-100 g CO_2 MJ^{-1}, red color:>100 g CO_2 MJ^{-1})

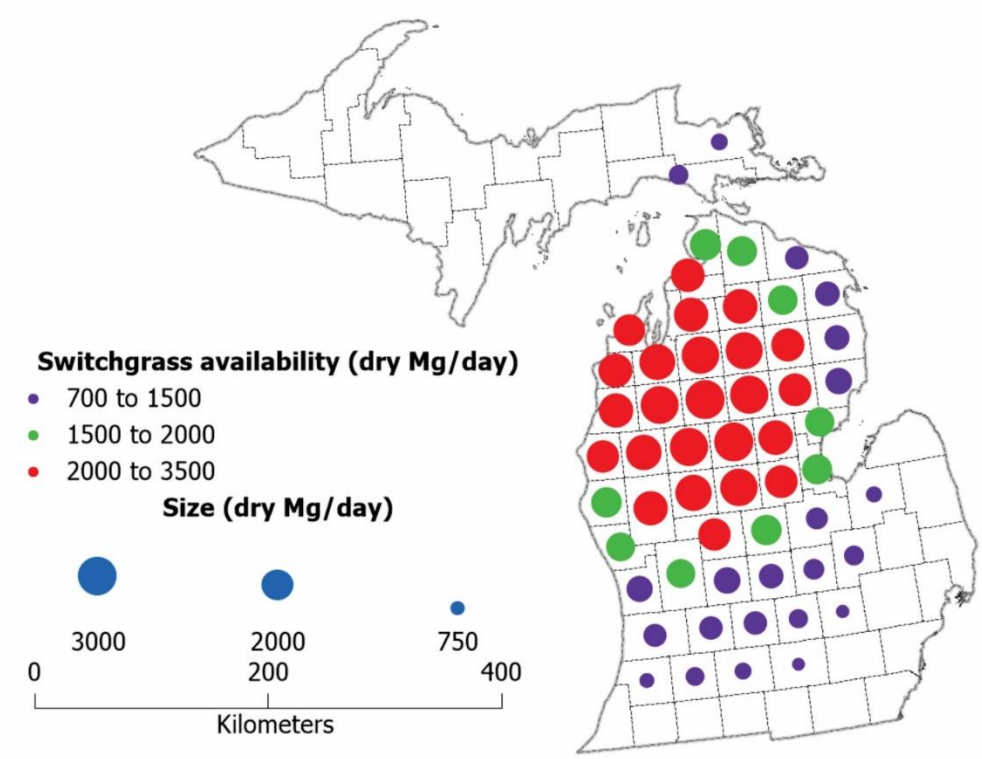

Figure S28. Switchgrass availability within a radius of 100 miles (161 km) of county centroids. [created with the Maptitude mapping software, www.caliper.com]

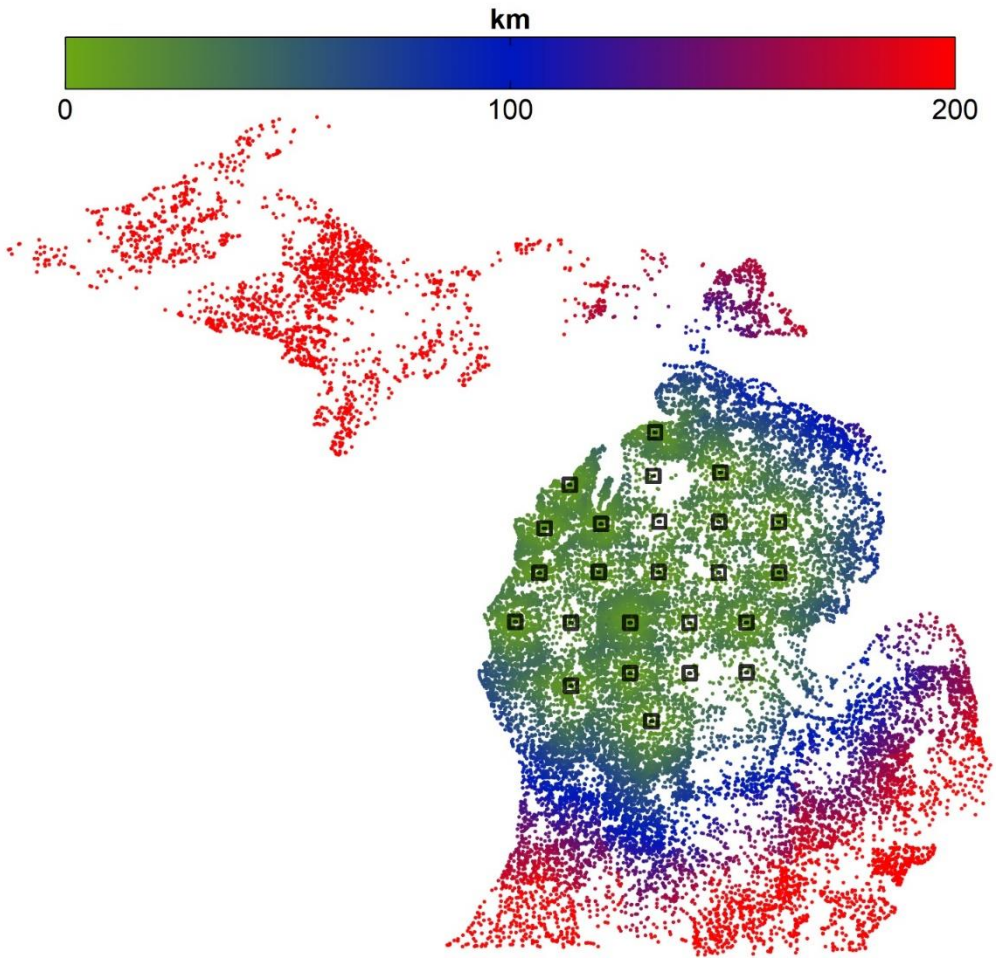

Figure S29. Minimum switchgrass transportation distance to county centroids with switchgrass availability greater than 2000 dry Mg day^{-1} within a 100-mile (161 km) radius (black colored square: centroid with switchgrass availability greater than 2000 dry Mg day^{-1}, red color:>200km)

References

1. U.S. Department of Energy (2016). 2016 Billion-Ton Report: Advancing Domestic Resources for a Thriving Bioeconomy, Volume 1: Economic Availability of Feedstocks (ORNL/TM-2016/160). Retrieved from https://www.energy.gov/eere/bioenergy/downloads/2016-billion-ton-report-advancing-domestic-resources-thriving-bioeconomy
2. Argonne National Laboratory (2020). The Greenhouse gases, Regulated Emissions, and Energy use in Transportation Model 2020.
3. Won, W.; Motagamwala, A. H.; Dumesic, J. A.; Maravelias, C. T., A co-solvent hydrolysis strategy for the production of biofuels: process synthesis and technoeconomic analysis. Reaction Chemistry & Engineering 2017, 2 (3), 397-405.

4. Tao, L., Schell, D., Davis, R., Tan, E., Elander, R., Bratis, A. (2014a). NREL 2012 Achievement of Ethanol Cost Targets: Biochemical Ethanol Fermentation via Dilute-Acid Pretreatment and Enzymatic Hydrolysis of Corn Stover. NREL/TP-5100-61563 United States 10.2172/1129271, National Renewable Energy Laboratory. Retrieved from https://www.osti.gov/servlets/purl/1129271
5. Chen, L., Blanc-Betes, E., Hudiburg, T.W., Hellerstein, D., Wallander, S., DeLucia, E.H., Khanna, M. (2021). Assessing the Returns to Land and Greenhouse Gas Savings from Producing Energy Crops on Conservation Reserve Program Land. Environmental science & technology, 55 (2), 1301-1309.